

Targeting TNF/IL-17/MAPK pathway in *hE2A-PBX1* leukemia: effects of OUL35, KJ-Pyr-9, and CID44216842

Haiping Luo,^{1*} Qiqi Li,^{1*} Jiaxin Hong,¹ Zhibin Huang,¹ Wenhui Deng,¹ Kunpeng Wei,¹ Siyu Lu,¹ Hailong Wang,² Wenqing Zhang¹ and Wei Liu¹

¹Division of Cell, Developmental and Integrative Biology, School of Medicine, South China University of Technology and ²KingMed School of Laboratory Medicine, Guangzhou Medical University, Department of Basic Research, Guangzhou Laboratory, Guangzhou, China

*HL and QL contributed equally as first authors.

Correspondence: W. Liu
liuwei7@scut.edu.cn

W. Zhang
mczhangwq@scut.edu.cn

Received: June 13, 2023.

Accepted: February 12, 2024.

Early view: February 22, 2024.

<https://doi.org/10.3324/haematol.2023.283647>

©2024 Ferrata Storti Foundation

Published under a CC BY-NC license



Abstract

t(1;19)(q23;p13) is one of the most common translocation genes in childhood acute lymphoblastic leukemia (ALL) and is also present in acute myeloid leukemia (AML) and mixed-phenotype acute leukemia (MPAL). This translocation results in the formation of the oncogenic E2A-PBX1 fusion protein, which contains a trans-activating domain from E2A and a DNA-binding homologous domain from PBX1. Despite its clear oncogenic potential, the pathogenesis of E2A-PBX1 fusion protein is not fully understood (especially in leukemias other than ALL), and effective targeted clinical therapies have not been developed. To address this, we established a stable and heritable zebrafish line expressing human *E2A-PBX1* (*hE2A-PBX1*) for high-throughput drug screening. Blood phenotype analysis showed that *hE2A-PBX1* expression induced myeloid hyperplasia by increasing myeloid differentiation propensity of hematopoietic stem cells (HSPC) and myeloid proliferation in larvae, and progressed to AML in adults. Mechanistic studies revealed that *hE2A-PBX1* activated the TNF/IL-17/MAPK signaling pathway in blood cells and induced myeloid hyperplasia by upregulating the expression of *runx1*. Interestingly, through high-throughput drug screening, three small molecules targeting the TNF/IL-17/MAPK signaling pathway were identified, including OUL35, KJ-Pyr-9, and CID44216842, which not only alleviated the *hE2A-PBX1*-induced myeloid hyperplasia in zebrafish but also inhibited the growth and oncogenicity of human pre-B ALL cells with E2A-PBX1. Overall, this study provides a novel *hE2A-PBX1* transgenic zebrafish leukemia model and identifies potential targeted therapeutic drugs, which may offer new insights into the treatment of E2A-PBX1 leukemia.

Introduction

t(1;19)(q23;p13) is the most common chromosomal translocation in leukemia, causing 5-7% of childhood ALL^{1,2} and also AML/MPAL.^{3,4} In ALL, E2A-PBX1 is not a primary ALL prognostic factor, but it is associated with poor response to therapy and short remission.⁵ ALL patients with E2A-PBX1 translocation appear to have a high risk of relapse, and this translocation is also associated with known high-risk clinical features, including elevated white blood cell counts at diagnosis and central nervous system leukemia.^{6,7} Furthermore, a previous study has shown that the E2A-PBX1 fusion gene can serve as an effective minimal residual disease (MRD) marker following induction chemotherapy, the relapse rate of patients with rapid early conversion to negative for this gene is relatively low.^{5,8} Reports based on sporadic cases have indicated that E2A-PBX1-positive patients also exhibit

high-risk clinical features, including high cell counts, high serum lactate dehydrogenase levels, and central nervous system (CNS) involvement.³ Although recent intensified treatment regimens and allogeneic hematopoietic stem cell transplantation have improved the prognosis of adult ALL patients with E2A-PBX1,⁹ its systemic toxicity and high cost should not be overlooked.

The E2A-PBX1 protein resulting from t(1;19)(q23;p13) fusion combines the N-terminal transactivation domain of E2A (also known as TCF3) and the C-terminal DNA-binding homologous domain of PBX1.¹⁰ As a major regulator of B-lymphocyte generation, E2A determines the differentiation of B-cell lineages,¹¹ also plays an important role in maintaining the hematopoietic stem cell pool and promoting the maturation of myelo-lymphoid and myelo-erythroid progenitors.¹² PBX1, a TALE (3-amino-acid loop extension) transcription factor, interacts with other members of the HOX family to enhance their DNA-binding

specificity and affinity.¹³ PBX1 not only plays an important role in regulating morphologic patterning, organogenesis, and hematopoiesis, but is also an important component of the protein complex that regulates the expression of developmental genes.¹⁴

The oncogenic role of E2A-PBX1 has been reported in both the myeloid and lymphoid systems of mice and cell lines. For example, the transduction of E2A-Pbx1 into mouse myeloid progenitor cells via retroviral vectors results in AML in mice.^{14,15} Adding granulocyte-macrophage colony-stimulating factor (GM-CSF), *E2A-Pbx1* can also immortalize myeloid progenitor cells *in vitro*.¹⁶ On the other hand, the specific induction of E2A-PBX1 expression in the mouse lymphoid system leads to T/B-ALL,¹⁷⁻¹⁹ and the injection of E2A-PBX1 pro-T cells into mice leads to T-ALL and AML.²⁰ Although the oncogenic potential of E2A-PBX1 is clear, its pathogenic mechanism has not been fully elucidated (especially in leukemias other than ALL). Currently, there are three main explanations for the mechanism underlying E2A-PBX1-induced leukemia: i) E2A-PBX1 oncoprotein may deregulate the expression of critical genes normally controlled by PBX/HOX/MEINOX complexes; ii) it alters the function of transcriptional co-activators; and iii) it impairs the function of wild-type (WT) E2A.²¹ Recently, a study using two pre-B ALL cell lines found that E2A-PBX1 can induce pre-B ALL by directly interacting with RUNX1 and co-activating the expression of oncogenes, including *RUNX1*.¹ This study strongly supports the gain-of-function oncogenic role of E2A-PBX1.¹ However, the mechanism by which E2A-PBX1 mediates AML oncogenesis is still unclear. More importantly, although studies have reported the development of potential drugs for E2A-PBX1 leukemia,^{22,23} clinically effective targeting drugs for E2A-PBX1 leukemia are still lacking.

In order to better understand the mechanisms behind E2A-PBX1-induced leukemia and develop effective targeted therapies, we constructed an inducible human-derived *E2A-PBX1* leukemia model using zebrafish. In zebrafish, just like in mammals, definitive hematopoietic stem cells (HSC) arise from the ventral wall of the dorsal aorta (VDA), which is equivalent to the aorta-gonad-mesonephros (AGM) in mammals.²⁴ These HSC then migrate into the caudal hematopoietic tissue (CHT), where they expand and subsequently colonize the kidney marrow, equivalent to the mammalian bone marrow, to generate hematopoietic cells throughout adulthood.²⁴ Zebrafish have proven to be an excellent model for studying hematopoietic disorders, particularly in extensive therapeutic compound screenings, due to their transparency, small size, short lifespan (2-3 years), high fecundity and genetic similarity to humans.²⁵ In recent years, the successful establishment of zebrafish patient-derived xenograft (zPDX) models has further advanced the use of zebrafish in biomedical research applications.^{26,27}

In our research, this hE2A-PBX1 transgenic zebrafish exhibited a phenotype of aberrant myeloid expansion and lymphoid dysplasia in larvae and eventually progressed to AML-like disease with age. Further mechanistic analysis revealed that hE2A-PBX1 activated the TNF/IL-17/MAPK signaling pathway in blood cells and induced myeloid hyperplasia by upregulating *runx1* expression. Importantly, through drug screening, we found that the small molecule compounds OUL35, KJ-Pyr-9 and CID44216842, which target the TNF/IL-17/MAPK signaling pathway, not only significantly alleviated the AML-like phenotype in the hE2A-PBX1 zebrafish model, but also blocked the oncogenicity of human E2A-PBX1 pre-B cells. In conclusion, our study provides insights into the mechanisms by which E2A-PBX1 causes AML-like disease and identifies several promising compounds for targeted therapy.

Methods

Generation of pT2AL-*hsp70*-hE2A-PBX1 construct and of *Tg(hsp70:E2A-PBX1-EGFP)* transgenic zebrafish

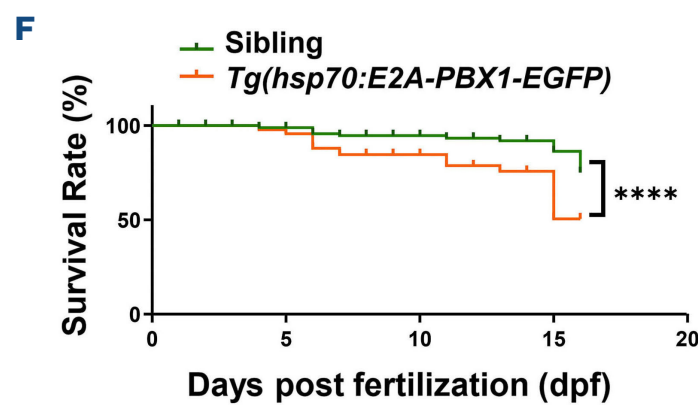
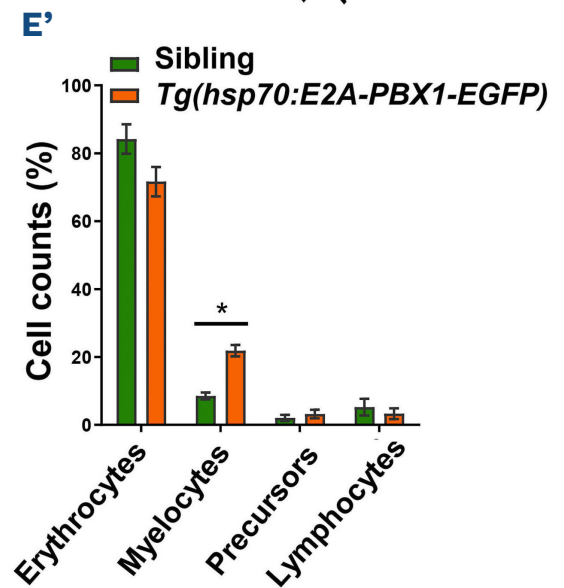
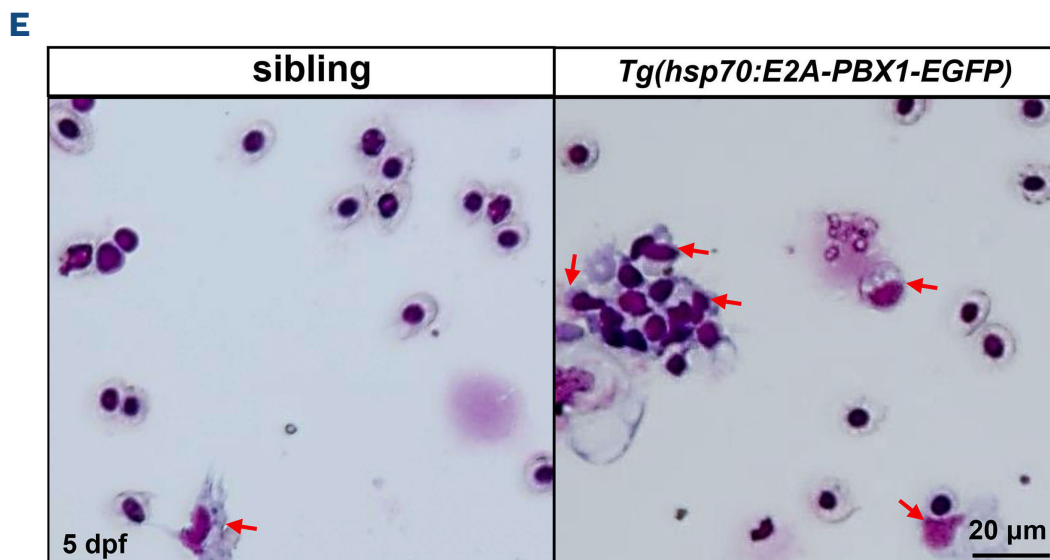
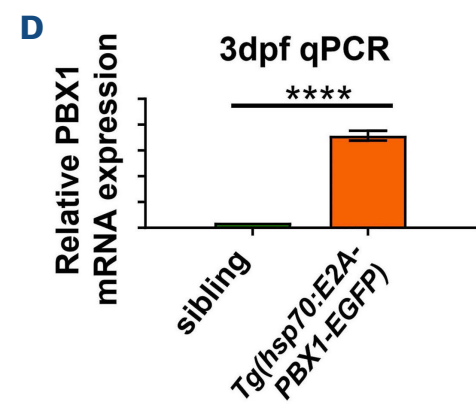
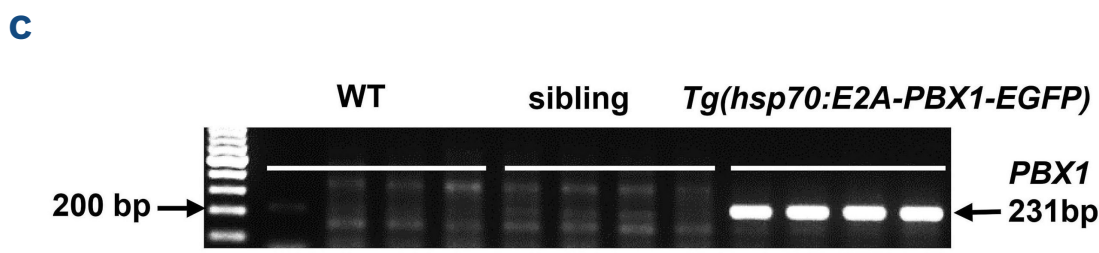
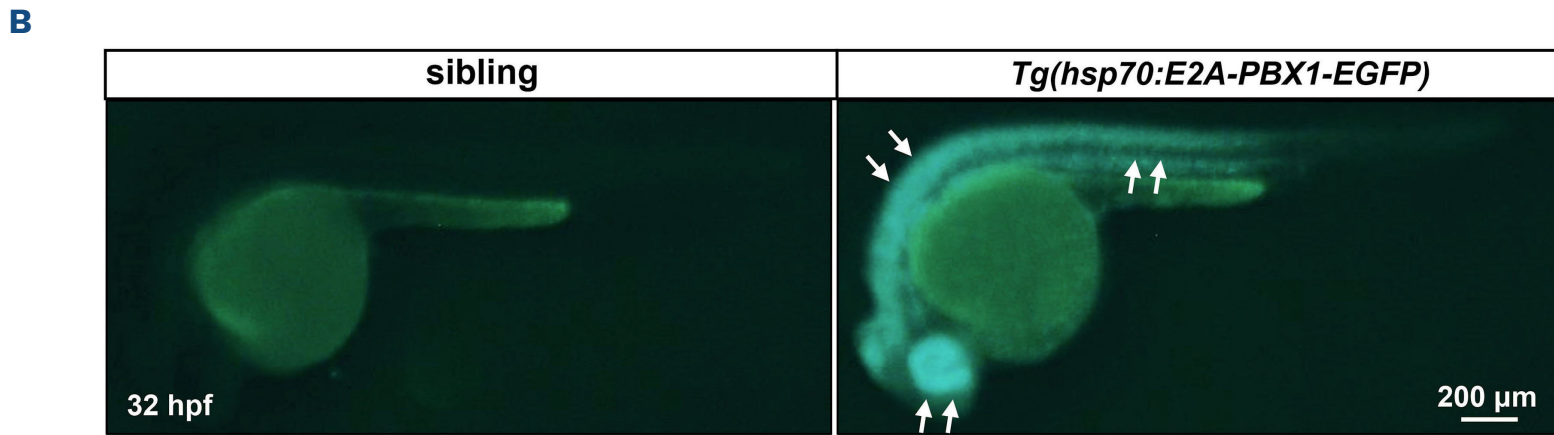
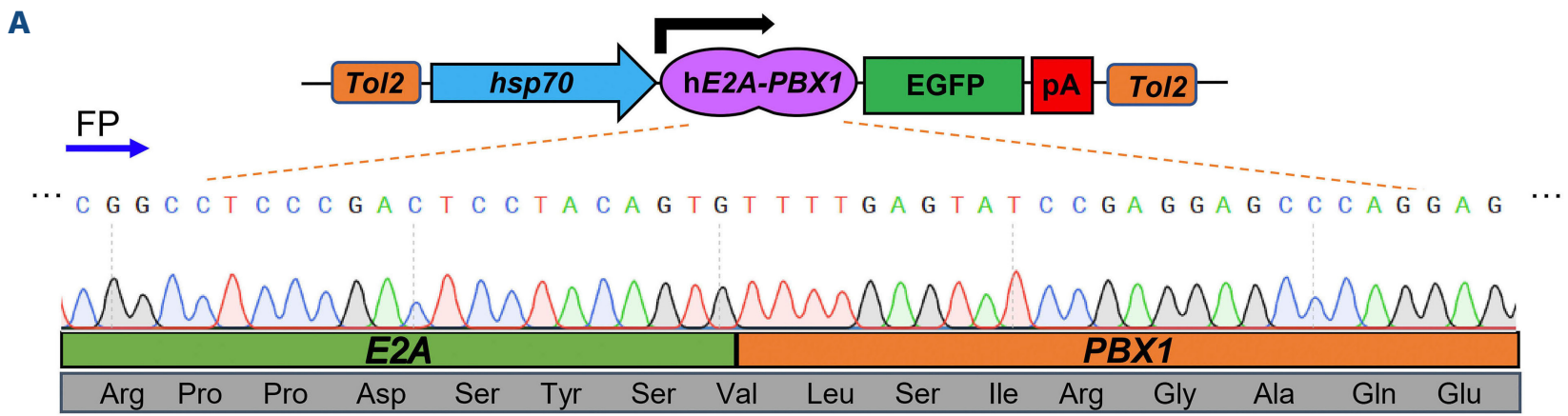
The pT2AL-*hsp70*-E2A-PBX1-EGFP plasmid is composed of *hsp70* promoter, a hE2A-PBX1 cDNA fragment obtained via polymerase chain reaction (PCR) from human samples, the Tol2 element and the SV40 poly A sequence. The *E2A* and *PBX1* cDNA fragments were linked together through overlap PCR. Following AgeI/SphI digestion, the hE2A-PBX1 sequence was inserted downstream of *hsp70* promoter and subcloned into the pT2AL plasmid. This construct, named pT2AL-*hsp70*-hE2A-PBX1-EGFP, was used for microinjection into zebrafish embryos at the one-cell stage along with Tol2 transposon mRNA to generate the *Tg(hsp70:E2A-PBX1-EGFP)* transgenic zebrafish.

Immunohistochemical staining

Abdominal tissue (above the pelvic fin) from euthanized adult fish was fixed in 4% paraformaldehyde (PFA) and subsequently processed into frozen sections,²⁸ permeabilized with 0.3% triton-X-100, and blocked with 5% fetal bovine serum. The sections were then incubated with rabbit-anti-Lcp1 monoclonal antibody (1:200),²⁹ followed by Alexa Fluor 488-anti-rabbit antibody (Invitrogen; 1:400) and DAPI (Invitrogen) for fluorescent visualization.

Bromodeoxyuridine labeling

Sibling and *Tg(hsp70:E2A-PBX1-EGFP)* embryos at 5-6 days post-fertilization (dpf) were incubated in 10 mM bromodeoxyuridine (BrdU) (Sigma-Aldrich) for 4 hours. The embryos were then stained with goat-anti-DsRed (Abcam; 1:400) and rabbit-anti-Lcp1 monoclonal antibody (1:200), followed by incubation with Alexa Fluor 488-anti-goat antibody (Invitrogen; 1:400) and Alexa Fluor 488-anti-rabbit antibody (Invitrogen; 1:400) for fluorescent visualization, according to the provided instructions.³⁰



Continued on following page.

Figure 1. Generation and characterization of transgenic zebrafish expressing human E2A-PBX1 (hE2A-PBX1). (A) Schematic representation of *Tg(hsp70:E2A-PBX1-EGFP)* expression vector, and Sanger sequencing confirmed the presence of the hE2A-PBX1 sequence. FP: forward primer; pA: poly A termination sequence. (B) F4 generation hE2A-PBX1-transgenic embryos exhibited EGFP expression at 32 hours post-fertilization (hpf). EGFP⁻ (sibling) and EGFP⁺ (*Tg(hsp70:E2A-PBX1-EGFP)*) embryos obtained by crossing the stable line *Tg(hsp70:E2A-PBX1-EGFP)* with wild-type (WT) fish. *Tg(hsp70:E2A-PBX1-EGFP)* embryos exhibited strong EGFP fluorescence (white arrows). (C) Specific polymerase chain reaction (PCR) amplification of a 231 bp fragment within the hE2A-PBX1 fusion region confirmed the integration of hE2A-PBX1 cDNA sequence into the genomes of *Tg(hsp70:E2A-PBX1-EGFP)*. (D) Real time quantitative PCR (RT-qPCR) analysis showed hE2A-PBX1 mRNA high expression in *Tg(hsp70:E2A-PBX1-EGFP)* compared to the siblings at 3 days post-fertilization (dpf). The black asterisks indicate statistical difference (Student *t* tests, mean \pm standard error of the mean; *****P*<0.0001) (E) Wright-Giemsa staining of whole blood cells from siblings and *Tg(hsp70:E2A-PBX1-EGFP)* at 5 dpf. Myelocytes are indicated by red arrows in the image. (E') Statistical analysis of the cell counts in panel (E). The black asterisks indicate statistical difference (one-way ANOVA, mean \pm standard error of the mean; **P*<0.05). N>150, number of zebrafish larvae. (F) Survival curves of *Tg(hsp70:E2A-PBX1-EGFP)* and sibling larvae up to 15 days after heat shock. The black asterisks indicate statistical difference (log-rank [Mantel-Cox] test; *****P*<0.0001).

TUNEL and immunofluorescence analyses

Transferase dUTP nick end labeling (TUNEL) assay (*In Situ* Cell Death Detection Kit; Roche) was performed as instructed. The samples were stained with goat-anti-DsRed (Abcam; 1:400) and rabbit-anti-Lcp1 antibody (1:200), followed by incubation with Alexa Fluor 488-anti-goat antibody (Invitrogen; 1:400) and Alexa Fluor 488-anti-rabbit antibody (Invitrogen; 1:400) for fluorescent visualization.

RNA-sequencing analysis

Whole kidney marrow (KM) cell suspensions were isolated from adult WT and *Tg(hsp70:E2A-PBX1-EGFP)*. RNA extraction was performed using TRIzol (Invitrogen),³⁰ and the extracted RNA samples were sent for library construction and RNA sequencing at Guangzhou Jidio Biotechnology.

Drug and inhibitor treatment

The small molecule inhibitors we screened were randomly selected from TargetMol's Bioactive Compound Library (*Online Supplementary Excel S1*). These compounds were all diluted to 20 mM as storage solution. KJ-Pyr-9, OUL35, A-484954, LRRK2-IN-1, CID44216842 were dissolved in dimethyl sulfoxide (DMSO), while L-arginine hydrochloride was dissolved in ddH₂O.

Animal care and xenograft procedure

Animal studies were performed in accordance with the animal research advisory committee of South China University of Technology. At 3 dpf, zebrafish larvae (*runx1^{w84x}*) were injected with 600 human leukemic cells per embryo through the yolk sac into the posterior cardinal vein (PCV) or dorsal aorta (DA).³¹⁻³³ The embryos were maintained at 35°C. On 1 day post-injection (dpi), zebrafish larvae were treated with the specified drug concentrations. Confocal microscopy was employed from 1 dpi to 4 dpi for image examination.

Statistical analysis

Statistical analysis was performed using GraphPad Prism version 6.000. Survival analysis utilized Kaplan-Meier (K-M) curves and the log-rank (Mantel-Cox) test. Student *t* tests compared two groups, and one-way analysis of variance

(one-way ANOVA) with Tukey's adjustment was used for multiple group comparisons. A significance level of *P*<0.05 was applied, and all data were presented as mean \pm standard error of the mean.

Results

Generation of an inducible humanized E2A-PBX1 transgenic zebrafish

In order to investigate the effects of humanized E2A-PBX1 on hematopoiesis, we created transgenic zebrafish with hE2A-PBX1 fusion gene expression controlled by the *hsp70* promoter. The pT2AL-*hsp70-E2A-PBX1-EGFP* plasmid with correct sequence (Figure 1A) was obtained after sequencing and microinjected into WT zebrafish to obtain the F0 generation (*Online Supplementary Figure S1A*). We obtained a diverse range of progeny by crossing the F0 with WT fish and identified a transgenic line (named: *Tg(hsp70:E2A-PBX1-EGFP)*) in the F4 generation, which stably inherited the transgene and exhibited strong EGFP fluorescence. After inducing the transgenic zebrafish with heat shock at 39.5°C, EGFP expression was observed in the whole body of 32 hpf embryos (Figure 1B). In addition, PCR detected a 231 bp human-derived *PBX1* target fragment in *Tg(hsp70:E2A-PBX1-EGFP)* transgenic zebrafish (Figure 1C), real time quantitative PCR (RT-qPCR) showed higher hE2A-PBX1 mRNA expression in *Tg(hsp70:E2A-PBX1-EGFP)* at 3 dpf (Figure 1D). These results demonstrate that we successfully constructed a heritable and stable *Tg(hsp70:E2A-PBX1-EGFP)* transgenic zebrafish lineage with induced expression of the hE2A-PBX1. Furthermore, qPCR analysis showed consistent expression of endogenous *tcf3a* and *tcf3b* (equivalent to human *E2A*) in both the embryonic tail hematopoietic tissue (CHT) and adult peripheral blood of *Tg(hsp70:E2A-PBX1-EGFP)* zebrafish (*Online Supplementary Figure S1B-D*). This suggests that *Tg(hsp70:E2A-PBX1-EGFP)* zebrafish maintain normal expression of endogenous *e2a* while overexpressing human *E2A-PBX1*. Next, to examine the potential effects of the hE2A-PBX1 oncoprotein on blood development in zebrafish, we collected whole blood from zebrafish at 5 dpf after heat shock and performed Giemsa staining. It was found that

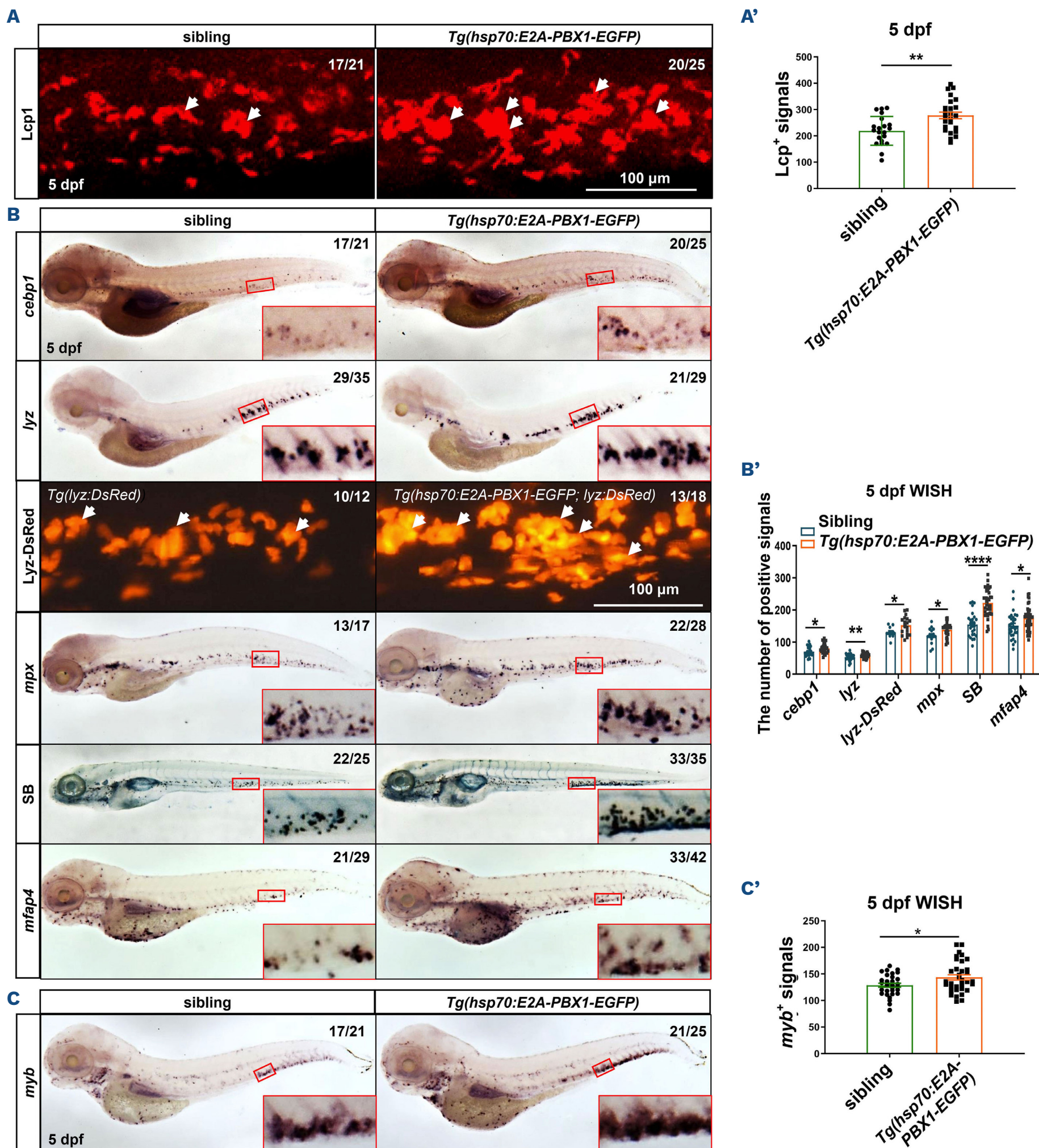


Figure 2. Induction of hE2A-PBX1 expression in zebrafish larvae leads to myeloid cell and hematopoietic stem cell expansion. (A) Immunofluorescence staining of Lcp1⁺ cells in siblings (left panel) and *Tg(hsp70:E2A-PBX1-EGFP)* (right panel) at 5 days post-fertilization (dpf). (A') Statistical analysis of the Lcp1⁺ signals in panel (A). The black asterisks indicate statistical difference (Student *t* tests, mean \pm standard error of the mean [SEM]; ***P*<0.01) (B) Whole mount *in situ* hybridization (WISH) of *cebp1*, *lyz*, *mpx* and *mfap4* expressions in *Tg(hsp70:E2A-PBX1-EGFP)* (right panel) were higher than siblings (left panel) at 5 dpf. The number of *lyz*-DsRed⁺ cells (caudal hematopoietic tissue [CHT] region and Sudan Black B-positive [SB⁺] cells in *Tg(hsp70:E2A-PBX1-EGFP)* (right) was higher than siblings (left) at 5 dpf. The CHT is enlarged in the red box (original magnification \times 200). (B') Statistical analysis of the positive signals (*cebp1*, *lyz*, *lyz*-DsRed, *mpx*, SB and *mfap4*) in panel (B). The black asterisks indicate statistical difference

Continued on following page.

(Student *t* tests, mean \pm SEM; * P <0.05, ** P <0.01, **** P <0.0001) (C) WISH of *myb* expressions in *Tg(hsp70:E2A-PBX1-EGFP)* (right panel) were higher than siblings (left panel) at 5 dpf. (C') Statistical analysis of the *myb*⁺ signals in panel (C). The black asterisks indicate statistical difference (Student *t* tests, mean \pm SEM; * P <0.05). N/N: number of zebrafish larvae showing representative phenotype/total number of zebrafish larvae examined.

the number of myeloid cells was significantly increased (Figure 1E, E'), indicating that transient induction of hE2A-PBX1 expression may disrupt the hematopoiesis in zebrafish. Additionally, survival analysis of *Tg(hsp70:E2A-PBX1-EGFP)* fish revealed a significant increase in mortality within 15 days following the induction of hE2A-PBX1 expression, in comparison to their siblings (Figure 1F).

hE2A-PBX1 induces abnormal expansion of myeloid cells in zebrafish larvae

In order to further explore the effect of hE2A-PBX1 expression on the development of different hematopoietic lineages, we detected the marker genes of each hematopoietic lineage in *Tg(hsp70:E2A-PBX1-EGFP)* transgenic zebrafish after heat shock by whole mount *in situ* hybridization (WISH) and specific staining. The results showed a significant increase in myeloid cells (*l-plastin*: a myeloid gene that marks granulocytes and macrophages, also known as *lcp1*) (Figure 2A, A'), which was consistent with the hemogram changes in zebrafish larvae (Figure 1E). Further assays of myeloid terminally differentiated granulocytes and macrophages revealed a significant increase in the number of immature granulocytes (*ceb1*), mature granulocytes (*lyz*, *mpx*, Sudan Black B [SB]) and macrophages (*mfap4*) in both 3 dpf and 5 dpf (Figure 2B, B'; *Online Supplementary S2A, A'*). As myeloid cells originate from HSPC;³⁴ we aimed to investigate whether the increased number of myeloid cells was caused by the tendency of HSPC toward the myeloid lineage or if there was an overall increase in HSPC leading to increased differentiation into various lineages? In order to address this question, we examined the changes of HSPC (*myb*), lymphocytes (*rag1*, *rag2*), and erythrocytes (*βe1*) in *Tg(hsp70:E2A-PBX1-EGFP)* after heat shock. The results showed that *myb*⁺ HSPC increased at 5 dpf (Figure 2C, C'), while the number of *rag1*⁺ and *rag2*⁺ lymphocytes decreased significantly (*Online Supplementary Figure S2B, B'*), and *βe1*⁺ erythrocytes showed no significant change (*Online Supplementary Figure S2C, C'*). These data suggest that hE2A-PBX1 expression may lead to myeloid expansion in zebrafish by increasing HSPC with myeloid differentiation potential.

In addition, it has been reported that the expression of *PBX1* maintains cell proliferation,²¹ while the E2A protein promotes cell differentiation and has anti-proliferation effect.³⁵ Therefore, we investigated whether hE2A-PBX1 influences the proliferation of myeloid and lymphocytes in *Tg(hsp70:E2A-PBX1-EGFP)*. The proliferation and apoptosis of myeloid/lymphocytes in *Tg(hsp70:E2A-PBX1-EGFP)* fish were examined after heat shock by co-staining with BrdU/

TUNEL and *Lcp1/Rag2*, respectively. The results showed a significant increase in the proportion of proliferating cells among *Lcp1*⁺ myeloid cells in 5 dpf *Tg(hsp70:E2A-PBX1-EGFP)* compared to the siblings (Figure 3A, 3A'), while the proportion of apoptotic cells showed a significant decrease (Figure 3B, B'). In contrast, *Rag2*⁺ lymphocytes showed a significant decrease in proliferation (*Online Supplementary Figure S3A, A'*), with no significant change in apoptotic cells (*Online Supplementary Figure S3B, B'*). These data suggest that expression of hE2A-PBX1 leads to abnormal myeloid expansion by increasing the myeloid differentiation potential of HSPC on the one hand and inducing myeloid hyperplasia on the other hand.

In order to investigate the potential relationship between myeloid expansion and early mortality in hE2A-PBX1 zebrafish, we treated heat-shocked hE2A-PBX1 fish with drugs capable of reducing myeloid proliferation, namely cytarabine³⁶⁻³⁸ and flavopiridol.^{39,40} The results showed that, compared to the DMSO-treated control group, both cytarabine and flavopiridol treatments significantly reduce the population of SB⁺ myeloid cells in hE2A-PBX1 fish (*Online Supplementary Figure S3C, C'*), and increase their survival rate (*Online Supplementary Figure S3D*). This suggests that myeloid cell proliferation may be one of the contributing factors to the elevated mortality in hE2A-PBX1 zebrafish.

Induction hE2A-PBX1 expression in adult zebrafish leads to an acute myeloid leukemia-like phenotype

In order to analyze whether induced expression of hE2A-PBX1 leads to blood tumors in adult zebrafish, we administered 1-month continuous heat shock to 3-month-old adult fish and collected peripheral blood (PB) cells and kidney marrow (KM) blood cells for Giemsa staining to detect hematological changes. Although 1 month of hE2A-PBX1 induction did not alter the hemogram in PB, it resulted in a significant increase in myeloid cells in KM (*Online Supplementary Figure S4A, A'*). We then extended the heat shock time to 3 months to determine whether the degree of myeloid expansion induced by hE2A-PBX1 is related to the induction time. The results showed that the longer expression of hE2A-PBX1 not only further exacerbated the myeloid expansion and lymphoid reduction in KM, but also resulted in mild myeloid hyperplasia in PB (*Online Supplementary Figure S4B, B'*). Since myeloid leukemia is commonly associated with the patient's age, we induced 3-month continuous expression of hE2A-PBX1 in 1-year-old zebrafish. We found that the AML-like phenotype was more pronounced in aged zebrafish after 3 months of hE2A-PBX1 induced compared to young zebrafish. In addition to the significant increase

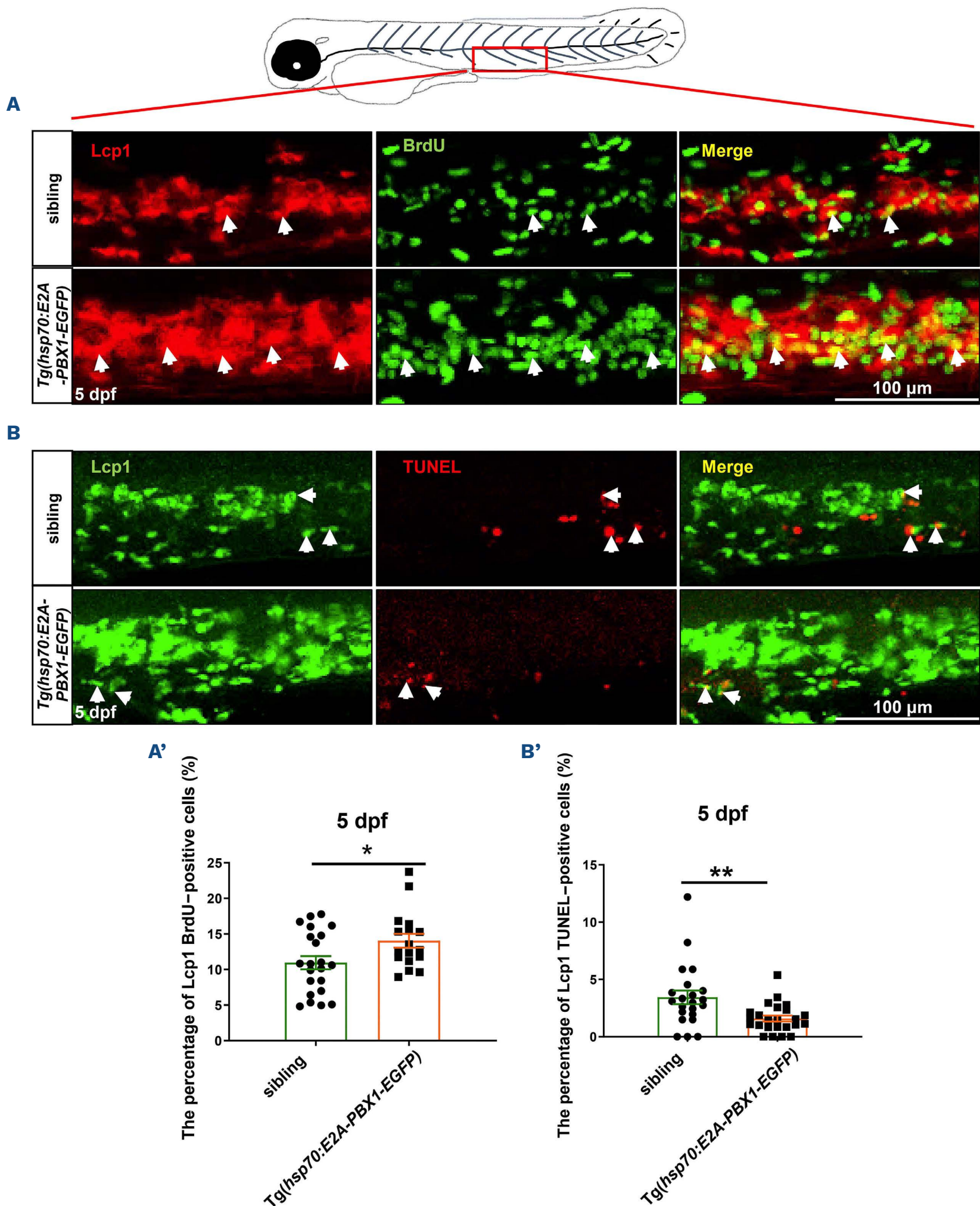


Figure 3. Abnormal myeloid cell expansion in *Tg(hsp70:E2A-PBX1-EGFP)* fish caused by proliferation and apoptosis perturbation.

(A) Immunofluorescence double staining of Lcp1 and bromodeoxyuridine (BrdU) antibodies reveals a significant increase in myeloid cell proliferation in the caudal hematopoietic tissue (CHT) region of 5 days post-fertilization (dpf) *Tg(hsp70:E2A-PBX1-EGFP)* larvae (N=22) compared with the siblings (N=17). Lcp1/BrdU double-positive cells are indicated by white arrows. (A') Statistical analysis of percentage of Lcp1⁺ BrdU⁺ cells in panel (A). The black asterisks indicate statistical difference (Student *t* tests, mean \pm standard error of the mean; **P*<0.05). (B) Co-staining of Lcp1 and transferase dUTP nick end labeling (TUNEL) was used to detect the apoptosis in the CHT region of 5 dpf *Tg(hsp70:E2A-PBX1-EGFP)* larvae (N=22) compared with the siblings (N=24). Lcp1/TUNEL double-positive cells are indicated by white arrows. (B') Statistical analysis of percentage of Lcp1⁺ TUNEL⁺ cells in panel (B). The black asterisks indicate statistical difference (Student *t* tests, mean \pm standard error of the mean; ***P*<0.01).

in myeloid cells and a further decrease in lymphocytes in KM, there was also a notable rise in myeloid blasts, and myeloid cells in PB showed a further increase (Figure 4A, A'; *Online Supplementary Figure S4C*). Furthermore, we ob-

served that the kidneys of *Tg(hsp70:E2A-PBX1-EGFP)* were significantly enlarged, and the enlargement worsened with the increase of hE2A-PBX1 expression and age (*data not shown*), especially in 1-year-old zebrafish with continuous

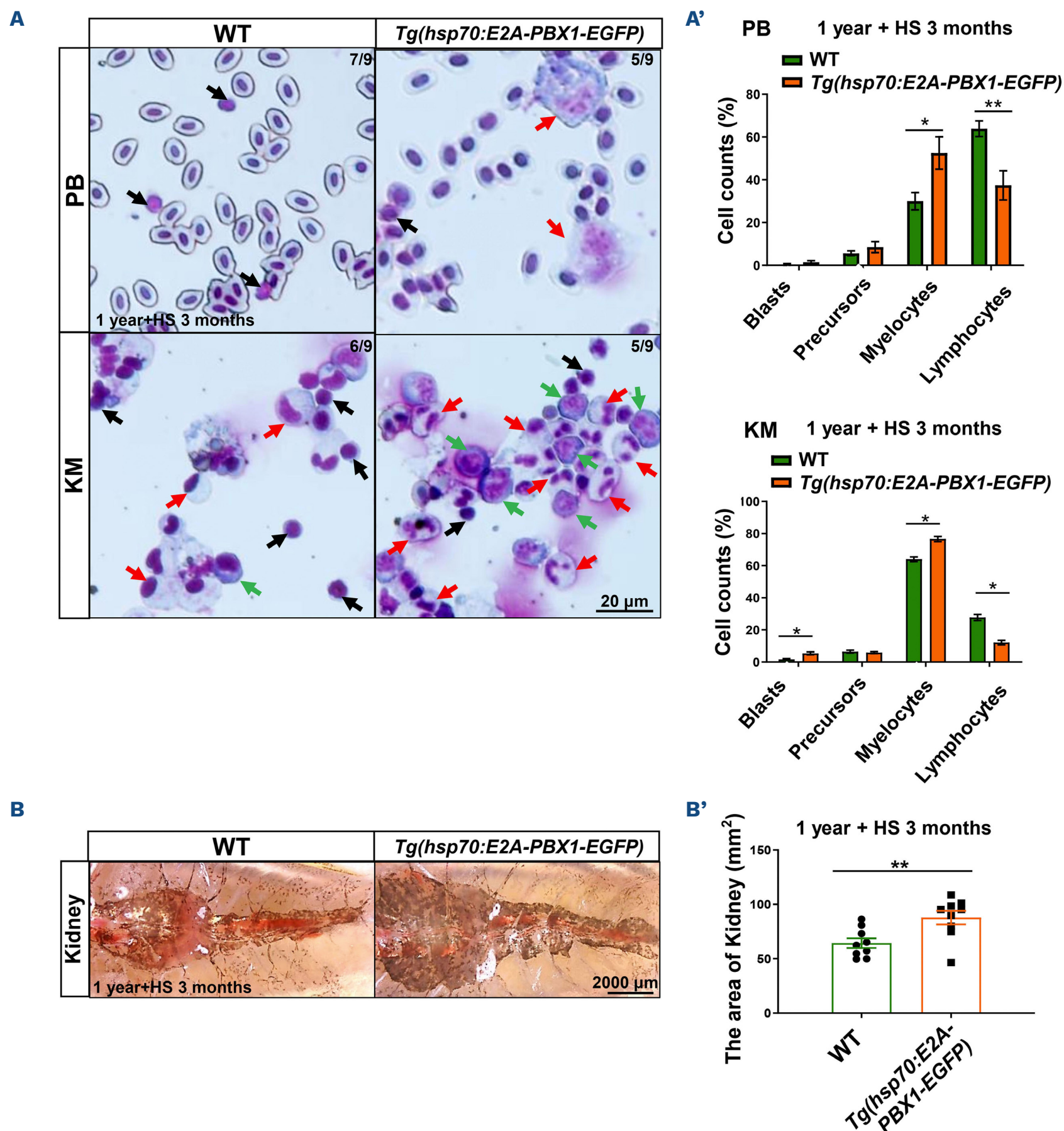


Figure 4. *Tg(hsp70:E2A-PBX1-EGFP)* adult fish exhibit abnormal myeloid cell expansion which resembles acute myeloid leukemia-like phenotypes. (A) May-Grunwald-Giemsa staining of peripheral blood (PB) cells (upper panels) and kidney marrow (KM) blood cells (lower panels) in 1-year-old wild-type (WT) (left panel) and *Tg(hsp70:E2A-PBX1-EGFP)* (right panel) adult fish after 3-month heat shock. Red arrows indicate myelocytes, black arrows indicate lymphocytes and green arrows indicate blasts. Original magnification $\times 400$. Blood cell counts of PB and KM were calculated manually based on their morphology. (A') Statistical analysis of cell counts in panel (A). The black asterisks indicate statistical difference (N=9, one-way ANOVA, mean \pm standard error of the mean; * $P < 0.05$, ** $P < 0.01$). (B) Kidneys from 1-year-old transgenic fish were enlarged to 1.36-fold in area compared with siblings after 3-month heat shock. (B') Statistical analysis of the area of kidney in panel (B). The black asterisks indicate statistical difference (N=9, Student *t* tests, mean \pm standard error of the mean; ** $P < 0.01$).

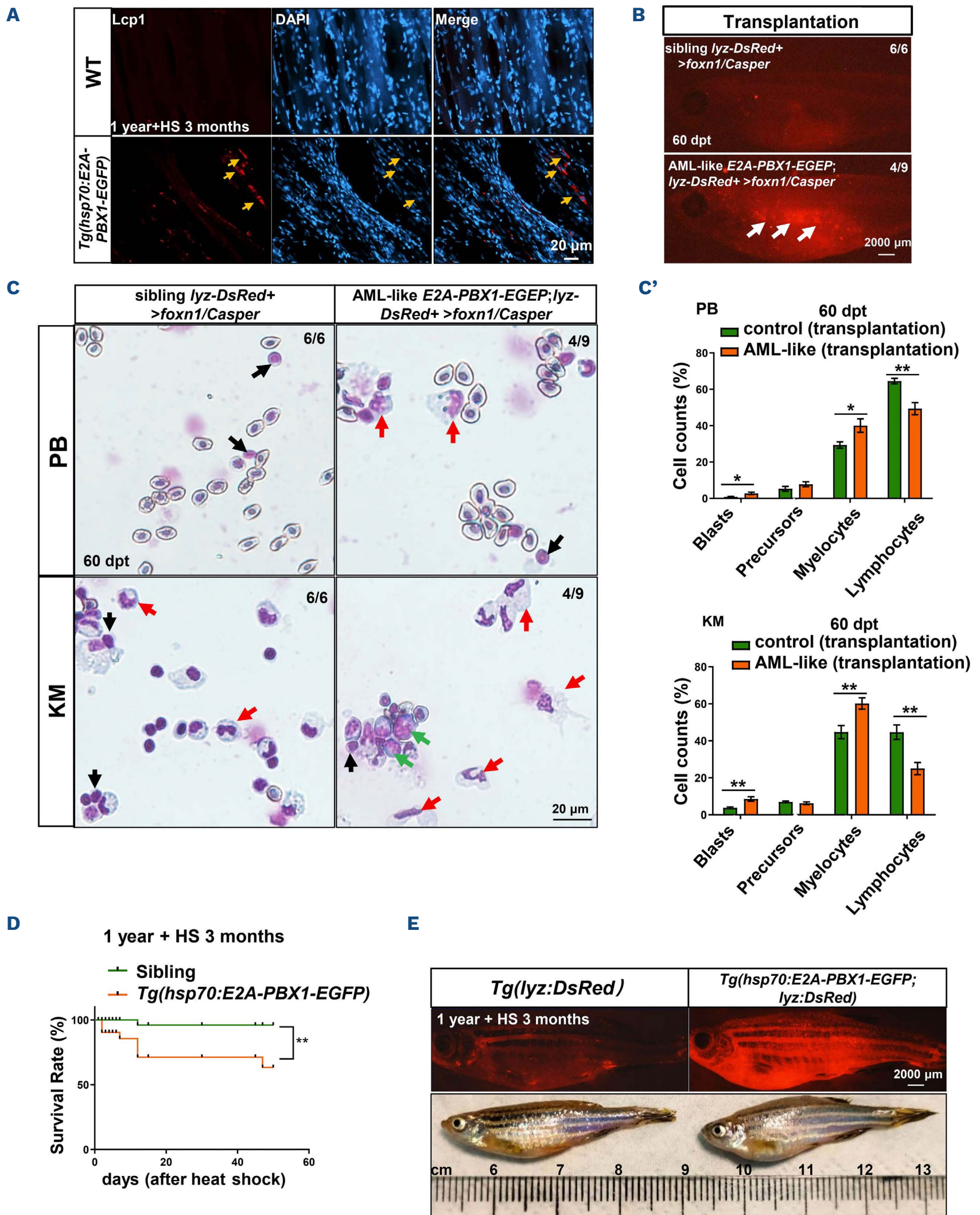


Figure 5. *Tg(hsp70:E2A-PBX1-EGFP;lyz:DsRed)* transgenic cells with induced acute myeloid leukemia-like disease are transplantable. (A) Immunofluorescent staining of the myeloid-specific marker Lcp1 in frozen sections confirmed myeloid cell invasion of the skeletal musculature in 1-year-old wild-type (WT) (left panel) and *Tg(hsp70:E2A-PBX1-EGFP)* (right panel) adult fish after 3-month heat shock (yellow arrows show invasion areas of myeloid cells into muscle tissue). (B) Direct observation of engrafted acute myeloid leukemia (AML)-like cells. At 60 days post-transplantation (dpt), AML-like *E2A-PBX1* *Lyz-DsRed+* cells could be visualized in *foxn1/Casper*-recipient kidney marrow (KM). The white arrow indicates the engrafted acute myeloid

Continued on following page.

leukemia (AML)-like *E2A-PBX1* Lyz-DsRed⁺ cells. N/N, number of zebrafish larvae showing representative phenotype/total number of zebrafish larvae examined. (C) Wright-Giemsa staining of blood cells in recipient KM after AML-like *E2A-PBX1* and WT Lyz-DsRed⁺ transplantation. The red arrows indicate the AML-like myelocytes, the green arrows indicate the blasts and the black arrows indicate lymphocytes in recipients. (C') Statistical analysis of cell counts in panel (C). The black asterisks indicate statistical difference (one-way ANOVA, mean \pm standard error of the mean; * $P < 0.05$, ** $P < 0.01$). (D) Survival curves of *Tg(hsp70:E2A-PBX1-EGFP)* and WT fish up to 90 day after heat shock. The black asterisks indicate statistical difference (log-rank [Mantel-Cox] test; ** $P < 0.01$). (E) Imaging of dying *Tg(hsp70:E2A-PBX1-EGFP;lyz:DsRed)* at 15-month-old after 3-month heat shock, reveals severe myeloid cell invasion.

3-month induction of hE2A-PBX1 (Figure 4B, B').

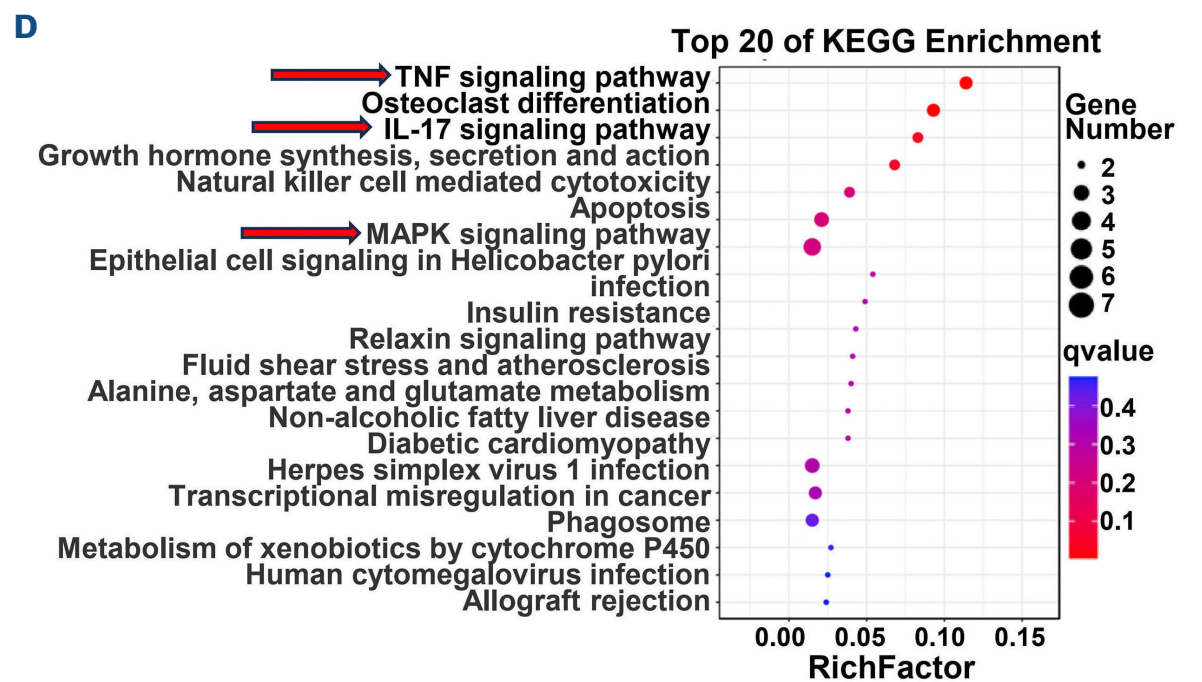
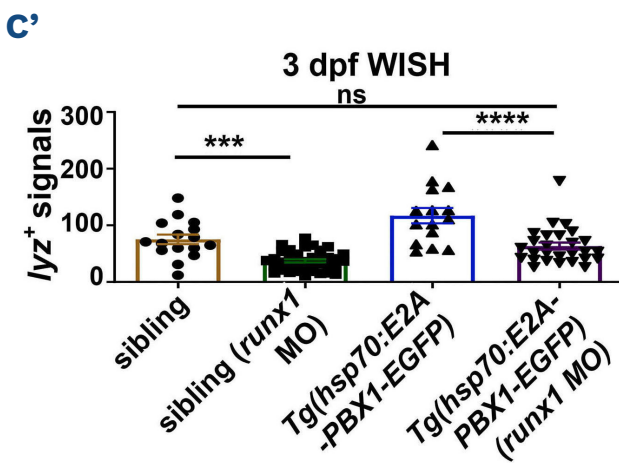
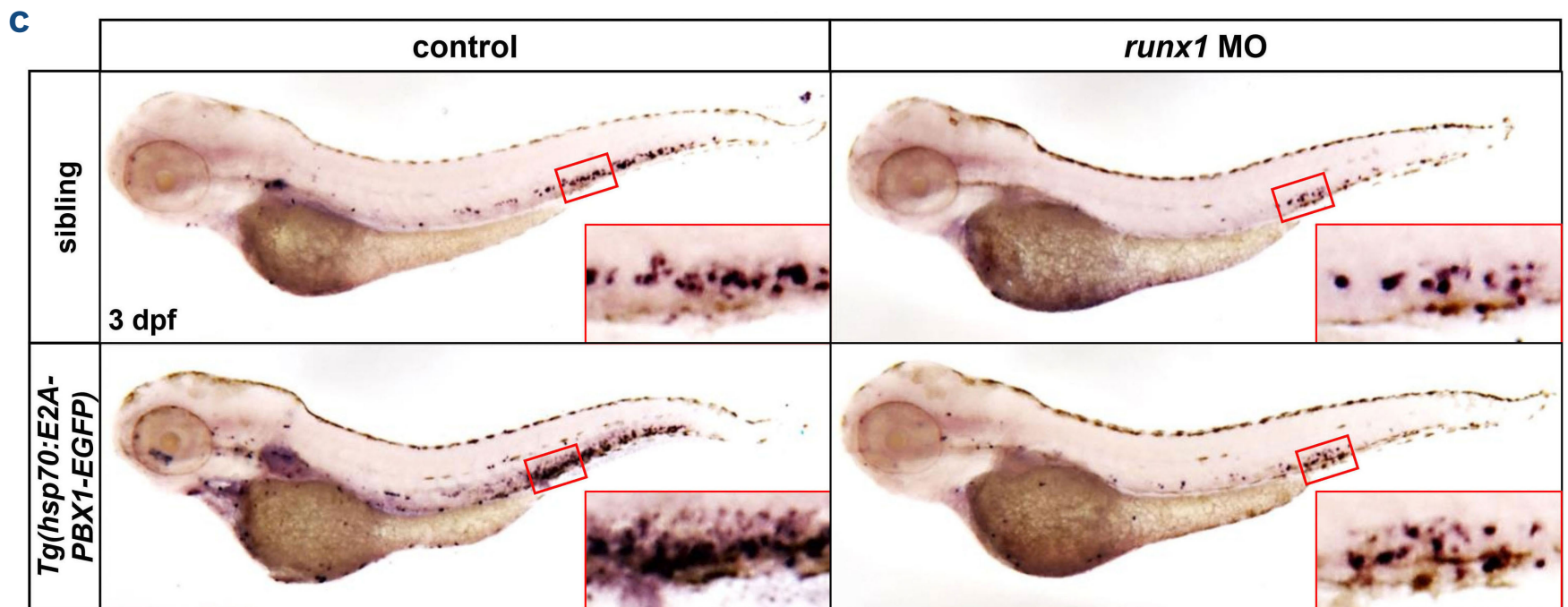
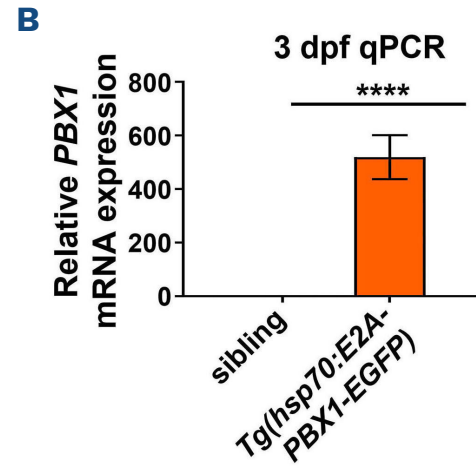
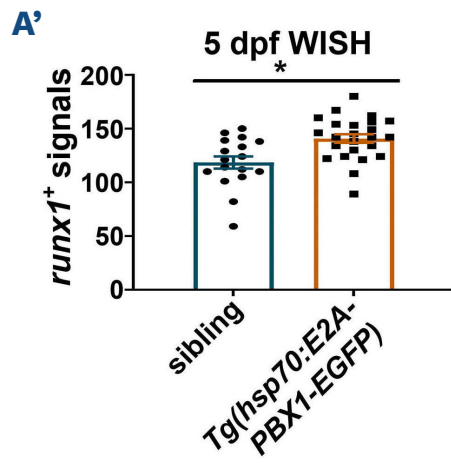
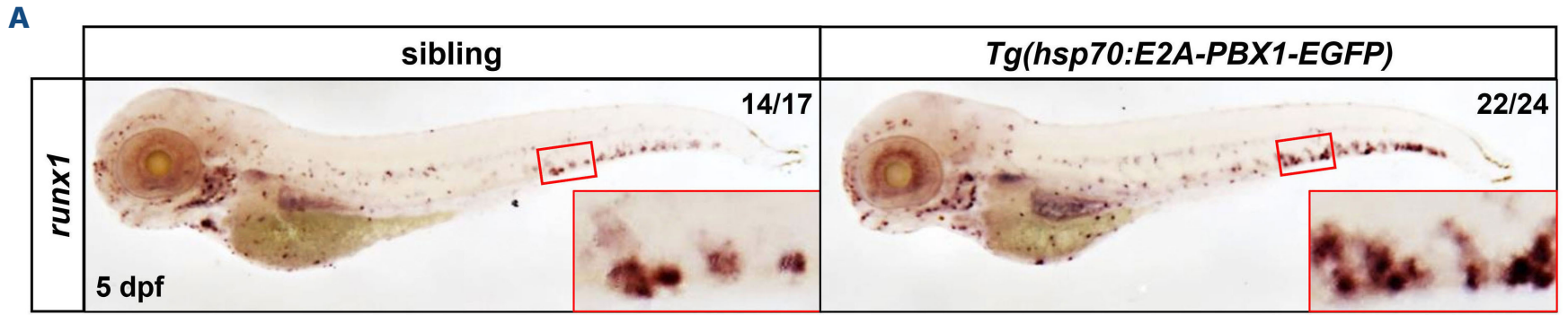
In order to clarify the malignancy of myeloid cells in *Tg(hsp70:E2A-PBX1-EGFP)*, we assessed the invasion of myeloid cells in the muscle after 3 month of heat shock in 3-month-old and 1-year-old zebrafish. The results showed a significant invasion of Lcp1⁺ myeloid cells in adult fish muscle after induction of hE2A-PBX1 expression compared with the control group (Figure 5A; *Online Supplementary Figure S5A*). Consistent with this, by using transgenic zebrafish, we observed pronounced systemic invasion of Lyz-DsRed⁺ myeloid cells in 1-year-old fish after 3 months of heat shock (*Online Supplementary Figure S5B*). We also detected substantial Lyz-DsRed⁺ myeloid cell invasion in the kidneys, liver, and spleen upon dissection of fresh tissues from adult zebrafish (*Online Supplementary Figure S5C*). In order to further confirm the transplantability of hE2A-PBX1-derived myeloid cells, we transplanted whole KM blood cells from *Tg(hsp70:E2A-PBX1-EGFP;lyz:DsRed)* zebrafish into immunocompromised adult host *foxn1/Casper* (*Online Supplementary Figure S5D*). The results revealed that 2 months after transplantation, compared to *Tg(-lyz:DsRed)* control donors, hE2A-PBX1-derived AML-like donor cells successfully repopulated *lyz-dsred*⁺ cells in the *foxn1/Casper* recipients (Figure 5B). Blood smears stained with Giemsa also showed a significant increase in myeloid cells and blasts in both peripheral blood (PB) and KM in recipients following AML-like fish KM transplants (Figure 5C, C'). Furthermore, survival analysis indicates that with the prolonged duration of heat shock, there is a gradual increase in mortality among 1-year-old hE2A-PBX1 zebrafish, accompanied by more severe systemic granulocytic invasion (Figure 5D, E). Taken together, our findings indicate that the induced expression of hE2A-PBX1 leads to myeloid expansion in adult fish and has the potential to progress to AML-like disease. Additionally, the degree of disease is positively correlated with the expression level of hE2A-PBX1 and the age of the animal.

hE2A-PBX1 induces myeloid expansion and activates TNF/IL-17/MAPK signaling pathway through upregulation of *runx1* expression

A recent *in vitro* study has shown that hE2A-PBX1 can activate oncogenes (including *RUNX1*), through direct interaction with *RUNX1* via *PBX1*, leading to the development of pre-B ALL.¹ In addition, mutations in *RUNX1* have been found to be a frequent cause of AML, T-ALL,

B-ALL, and myelodysplastic syndrome in clinical.⁴¹ In order to investigate whether hE2A-PBX1 causes AML-like symptoms are related to its regulation of *runx1*, we examined the expression level of *runx1* in *Tg(hsp70:E2A-PBX1-EGFP)* after heat shock by WISH and qPCR. The results showed that the expression level of *runx1* in transgenic zebrafish at 3 dpf and 5 dpf dpf after heat shock was significantly increased compared to the control group (Figure 6A, A', B). In order to further investigate the role of *Runx1* in hE2A-PBX1-induced myeloid expansion, we crossed *Tg(hsp70:E2A-PBX1-EGFP)* with the *runx1* loss-of-function mutant (*runx1^{w84x}*) to obtain *Tg(hsp70:E2A-PBX1-EGFP); runx1^{w84x}* embryos and detected the number of *lyz*⁺ granulocytes. The results showed a significant reduction in the number of granulocytes in both the sibling and hE2A-PBX1 transgenic zebrafish after *runx1* deletion (*Online Supplementary Figure S6A, A'*). Additionally, to investigate the dose-dependent relationship between the expression level of *runx1* and the number of granulocytes, we used the reported *runx1* morpholino (MO) to knock down *runx1* gradient (injection concentration: 0.7 mM, 0.5 mM, 0.2 mM) and detected the number of *lyz*⁺ granulocytes by WISH. Our results showed that the reduction in granulocytes was similar to that of *runx1^{w84x}* when injected at a concentration of 0.7 mM (*Online Supplementary Figure S6B, B'*), while restoring granulocyte numbers to sibling levels when injected at 0.2 mM (Figure 6C, C'), with intermediate levels observed at 0.5 mM (*data not shown*). These results suggest that hE2A-PBX1 induces myeloid expansion by upregulating *Runx1* expression. Further, we found that deletion of one allele of *runx1* in hE2A-PBX1 zebrafish (*Tg(hsp70:E2A-PBX1; runx1^{w84x/+})*) increased survival to a level similar to that of siblings, whereas overexpression (*Tg(hsp70:E2A-PBX1-EGFP; hsp70:myc-runx1)*) did not further exacerbate mortality in hE2A-PBX1 zebrafish (*Online Supplementary Figure S6C*). This is possibly because hE2A-PBX1 transgenic zebrafish already have extremely high levels of *runx1* expression, and further elevating *runx1* levels may not lead to additional mortality.

In order to further explore the effect of upregulation of *runx1* expression on hematopoietic transcription regulation in the hE2A-PBX1 transgenic line, we performed RNA sequencing analysis on blood cells of KM from 3-month-old *Tg(hsp70:E2A-PBX1-EGFP)* after 3-month continuous heat shock. The results showed that the TNF/



Continued on following page.

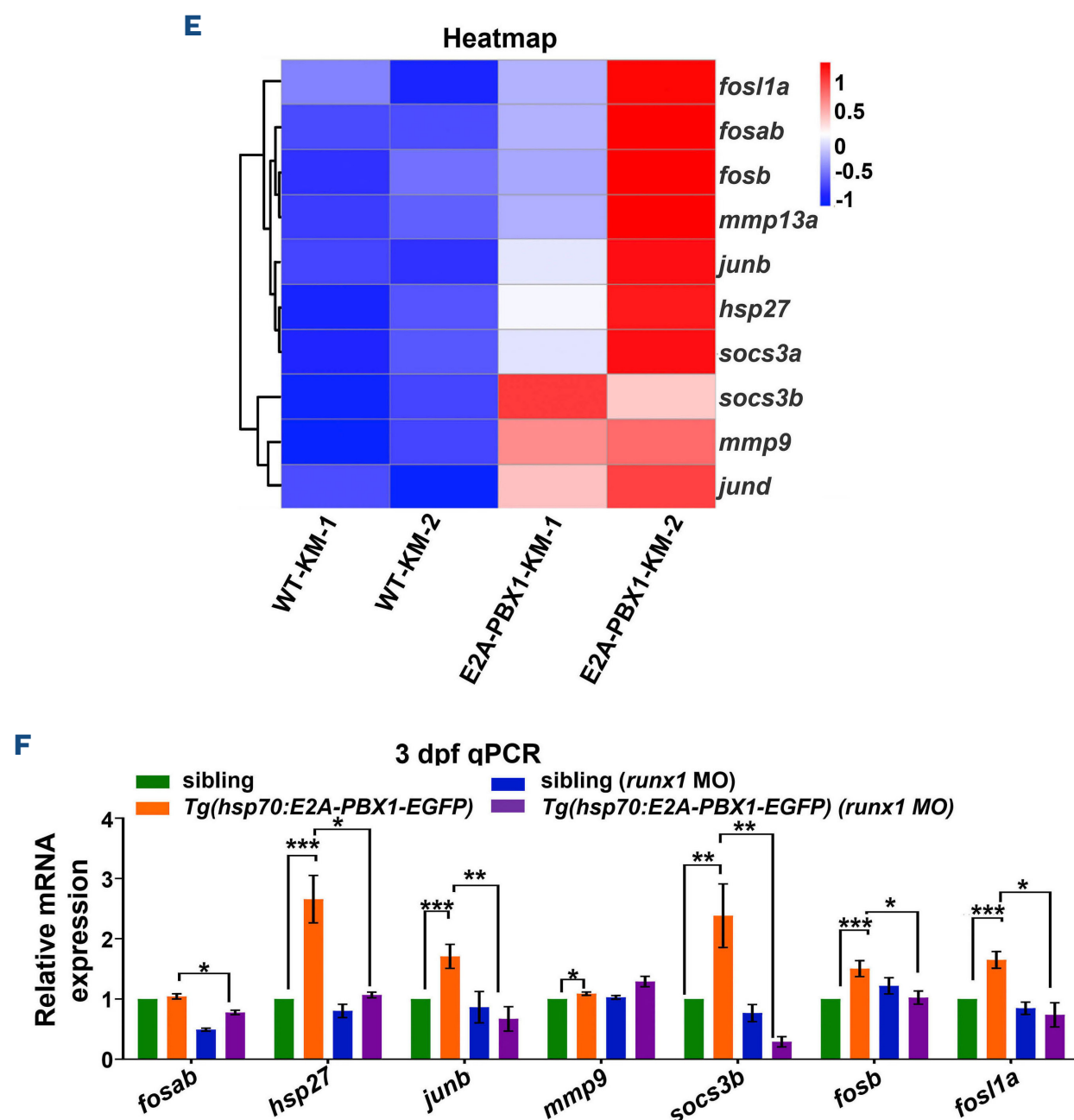


Figure 6. hE2A-PBX1 activate the TNF/IL-17/MAPK signaling pathway through upregulation of *runx1* expression. (A) Whole mount *in situ* hybridization (WISH) of *runx1* expressions in *Tg(hsp70:E2A-PBX1-EGFP)* (right panel) were higher than siblings (left panel) at 5 days post-fertilization (dpf). The caudal hematopoietic tissue (CHT) is enlarged in the red box (original magnification $\times 200$). (A') Statistical analysis of the *runx1*⁺ signals in panel (A). The black asterisks indicate statistical difference (Student *t* tests, mean \pm standard error of the mean [SEM]; **P*<0.05). N/N: number of zebrafish larvae showing representative phenotype/total number of zebrafish larvae examined. (B) Real time quantitative polymerase chain reaction (RT-qPCR) analysis showed increased *runx1* mRNA expression in *Tg(hsp70:E2A-PBX1-EGFP)* compared to the sibling controls at 3 dpf. The black asterisks indicate statistical difference (Student *t* tests, mean \pm SEM; *****P*<0.0001) (C) Decreased number of *lyz*⁺ neutrophils in sibling and *Tg(hsp70:E2A-PBX1-EGFP)* larvae after injecting 0.2 mM *runx1* morpholino (MO) at 3 dpf. The control groups were treated with 0.2 mM random sequence MO. The CHT is enlarged in the red box (original magnification $\times 200$). (C') Statistical analysis of the *lyz*⁺ signals shown in panel (C). The black asterisks indicate statistical difference (N \geq 15, one-way ANOVA, mean \pm SEM; ****P*<0.001, *****P*<0.0001). (D) Top 20 enriched KEGG pathways identified in the analysis of differentially expressed genes (DEG) in KM cells from 6-month-old *Tg(hsp70:E2A-PBX1-EGFP)* compared to control groups after 3-month heat shock. The TNF/IL-17/MAPK signaling pathway is highlighted by the red arrow. (E) Heatmap of DEG involved in the TNF/IL-17/MAPK signaling pathway between WT and hE2A-PBX1 adult fish. Red and blue represent an increase and decrease gene expression levels, respectively; *P*<0.05. (F) RT-qPCR analysis showing mRNA expression of *fosab*, *hsp27*, *junb*, *mmp9*, *socs3b*, *fosb* and *fosl1a* in *Tg(hsp70:E2A-PBX1-EGFP)* compared to siblings after injecting 0.2 mM *runx1* MO at 3 dpf. The control groups were treated with 0.2 mM random sequence MO (one-way ANOVA, mean \pm SEM; **P*<0.05, ***P*<0.01, ****P*<0.001). TNF: tumor necrosis factor; IL-17: interleukin-17; MAPK: mitogen-activated protein kinase.

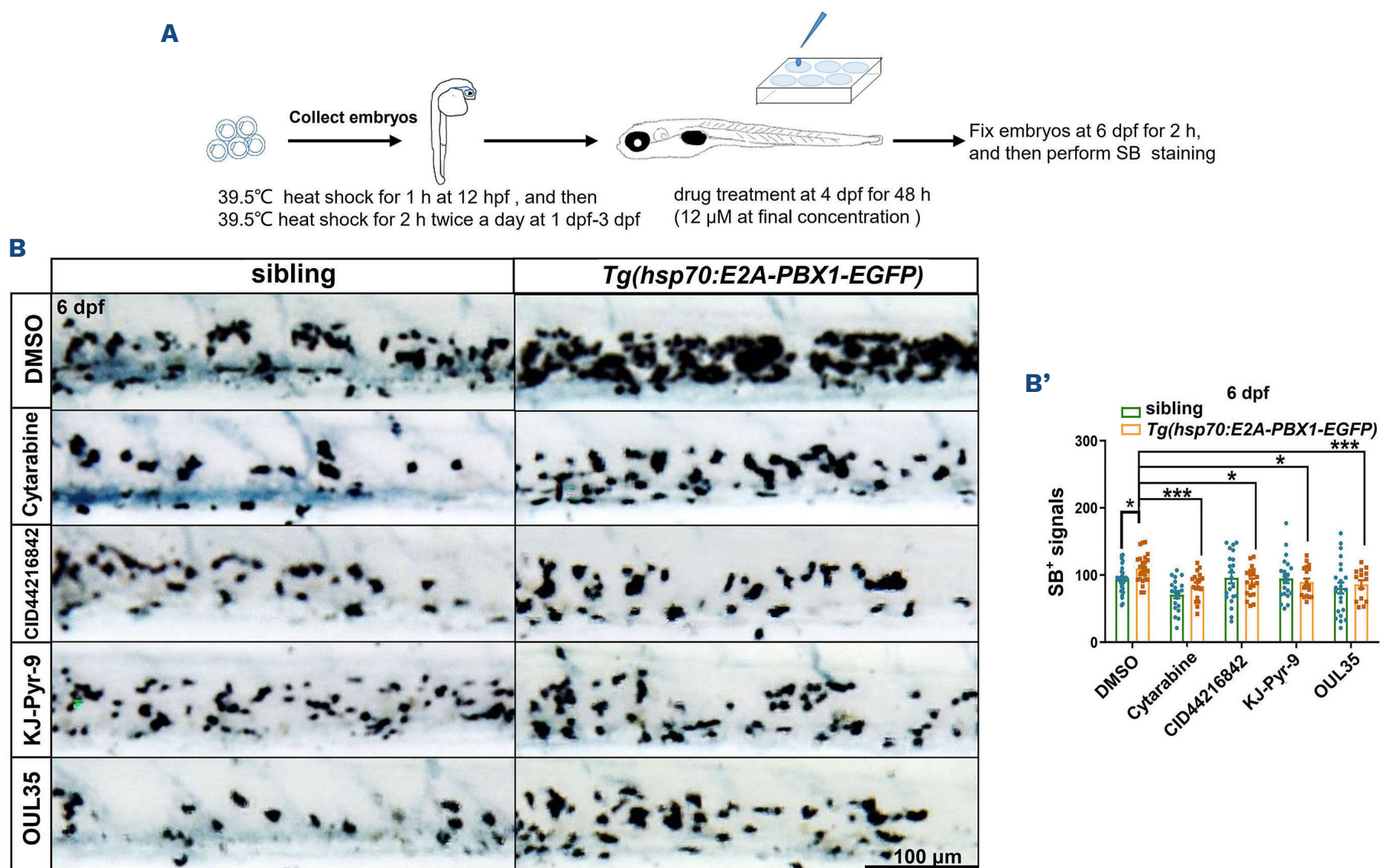
IL-17/MAPK signaling pathway was enriched in hE2A-PBX1 zebrafish (Figure 6D), with ten genes (*fosl1a*, *fosab*, *fosb*, *mmp13a*, *junb*, *hsp27*, *socs3a*, *socs3b*, *mmp9* and *jund*) were significantly upregulated in these pathways (Figure 6E). Additionally, we microinjected sibling and hE2A-PBX1 transgenic zebrafish with 0.2 mM *runx1* MO, and detected the changes of significantly upregulated genes in the TNF/

IL-17/MAPK signaling pathway after knockdown of *runx1*. The results showed that knockdown of *runx1* could significantly reverse the high expression of *hsp27*, *junb*, *socs3b*, *fosb* and *fosl1a* in hE2A-PBX1 transgenic line (Figure 6F). These data suggest that hE2A-PBX1 can induce myeloid expansion and activate the TNF/IL-17/MAPK signaling pathway through upregulation of *runx1* expression.

KJ-Pyr-9, OUL35, and CID44216842 effectively alleviate hE2A-PBX1-induced myeloid expansion in zebrafish

In order to identify small molecule compounds that can target hE2A-PBX1, we screened 560 small molecule inhibitors using *Tg(hsp70:E2A-PBX1-EGFP)* zebrafish. After 3 days of heat shock, embryos of *Tg(hsp70:E2A-PBX1-EGFP)* were collected and treated with drugs on day 4 (initial screening concentration was 12 μ M), and then fixed at 6 dpf to detect the number of SB⁺ granulocytes (Figure 7A). From the initial screening, we obtained seven small molecule inhibitors that significantly reduced the number of SB⁺ granulocytes in a concentration gradient of 8 μ M, 14 μ M, 20 μ M and 24 μ M (Online Supplementary Table S1). Interestingly, these seven drugs not only include L-arginine hydrochloride targeting inflammatory pathways, A-484954 and GLPG1837 targeting autophagy pathways, LRRK2-IN-1 targeting apoptosis pathways, but also include CID4421684, OUL35 and KJ-Pyr-9 targeting TNF/IL-17/MAPK, which is consistent with our previous finding that hE2A-PBX1 can activate the TNF/IL-17/MAPK signaling pathway in zebrafish (Figure 6D). In order to compare the effects of these three drugs with the existing chemotherapeutic drug Ara-C (cytarabine), we treated hE2A-PBX1 zebrafish with 6.17 mM Ara-C, 8 μ M KJ-Pyr-9, 20 μ M CID44216842 and 24 μ M of OUL35, respectively. The results showed that all three inhibitors reduced the number of SB⁺ granulocytes to the same ex-

tent as Ara-C (Figure 7B, B'), but OUL35 and CID44216842 exhibited a lower embryo deformity rate (Online Supplementary Figure S7A). Consistently, intraperitoneal injection of adult fish with cytarabine (8,000 mg/kg), CID44216842 (125 mg/kg), KJ-Pyr-9 (90 mg/kg), and OUL35 (150 mg/kg) for 5 consecutive days significantly reduced the proportion of myeloid cells in the KM (Online Supplementary Figure S7B, B'). Additionally, KJ-Pyr-9, OUL35, and CID44216842 also lowered the blast percentage in the KM. These findings indicate that KJ-Pyr-9, OUL35, and CID44216842 can alleviate the myeloid expansion in hE2A-PBX1 fish. Further, by long-term drug treatment (administration for 7 consecutive days) of hE2A-PBX1 zebrafish at 5 dpf, we found that cytarabine, CID44216842 and OUL35 could significantly improve the survival rate of hE2A-PBX1 zebrafish (Online Supplementary Figure S7C). KJ-Pyr-9 did not improve the death of hE2A-PBX1 zebrafish, which may be due to other side effects caused by long-term treatment of KJ-Pyr-9. It has been reported that TNF⁴²⁻⁴⁴ and IL-17⁴⁵⁻⁴⁷ can activate the MAPK pathway. In order to investigate whether TNF/IL-17 can similarly activate the MAPK signaling in *Tg(hsp70:E2A-PBX1-EGFP)*, we treated 4 dpf hE2A-PBX1 embryos with TNF- α inhibitors pomalidomide and lenalidomide, as well as IL-17 inhibitor Y-320. After 48 hours, we examined the activation of the MAPK pathway, expression of downstream target genes, and changes in SB⁺ myeloid cell numbers.



Continued on following page.

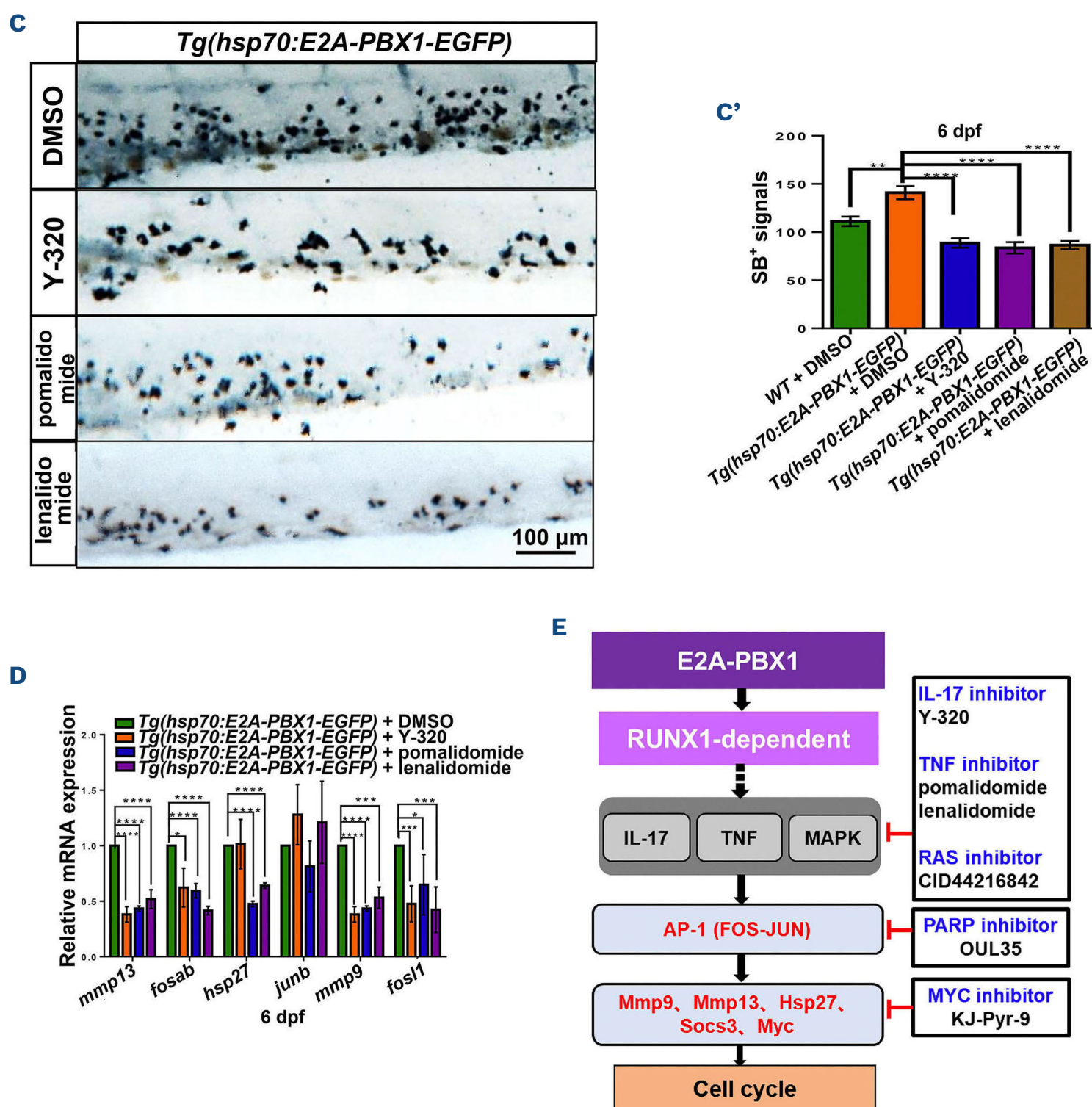
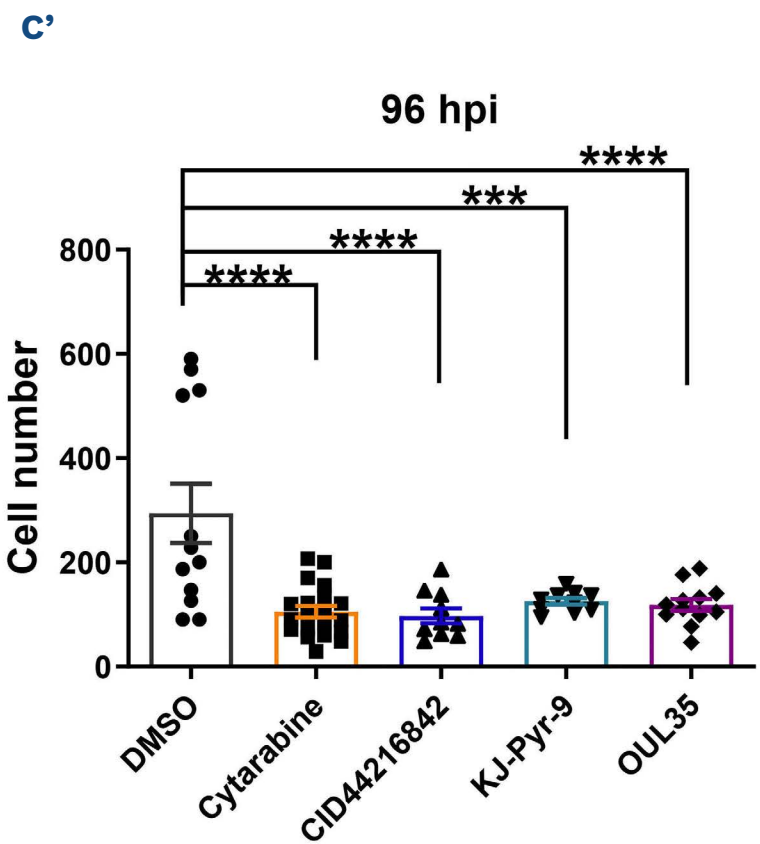
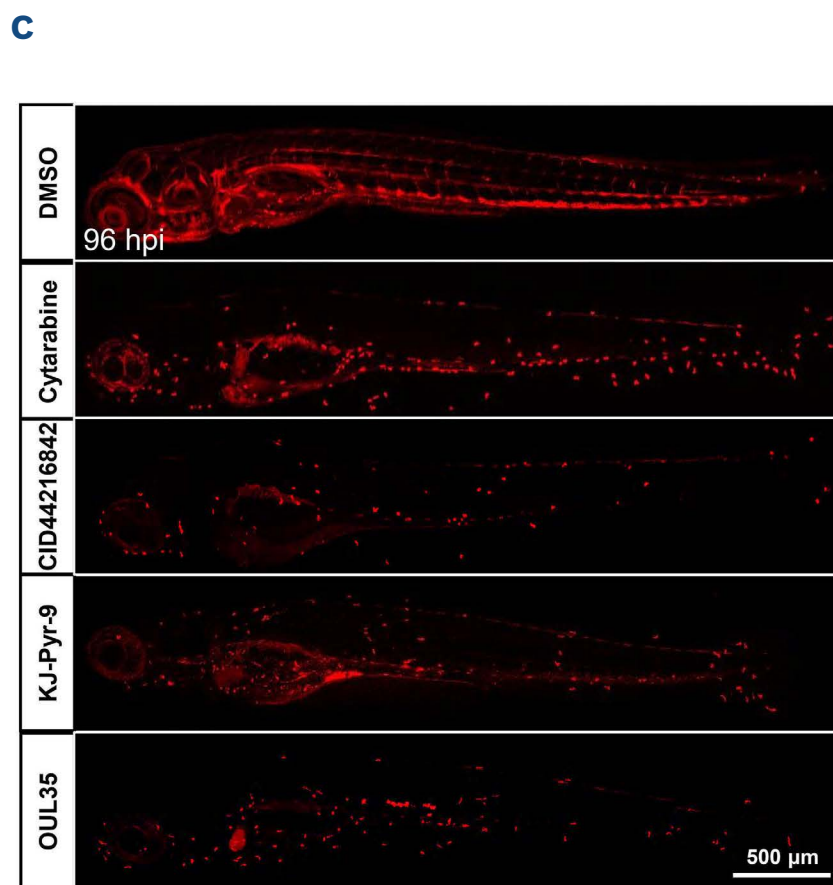
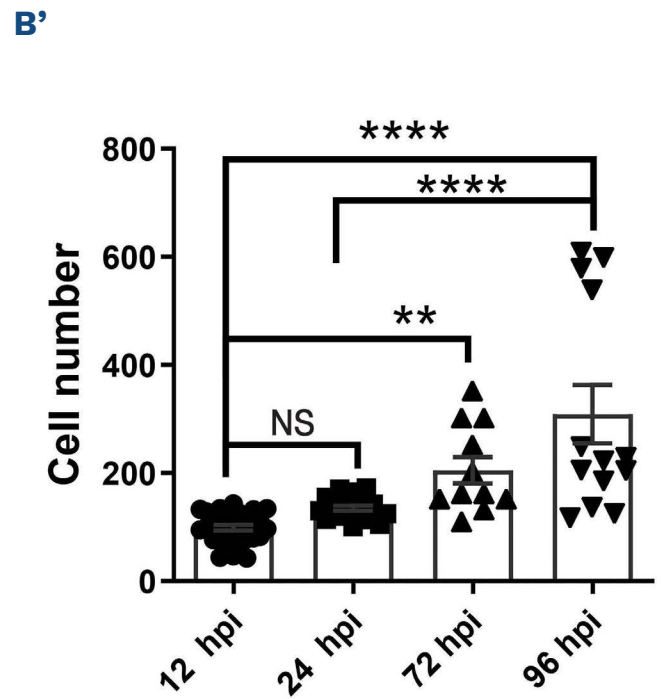
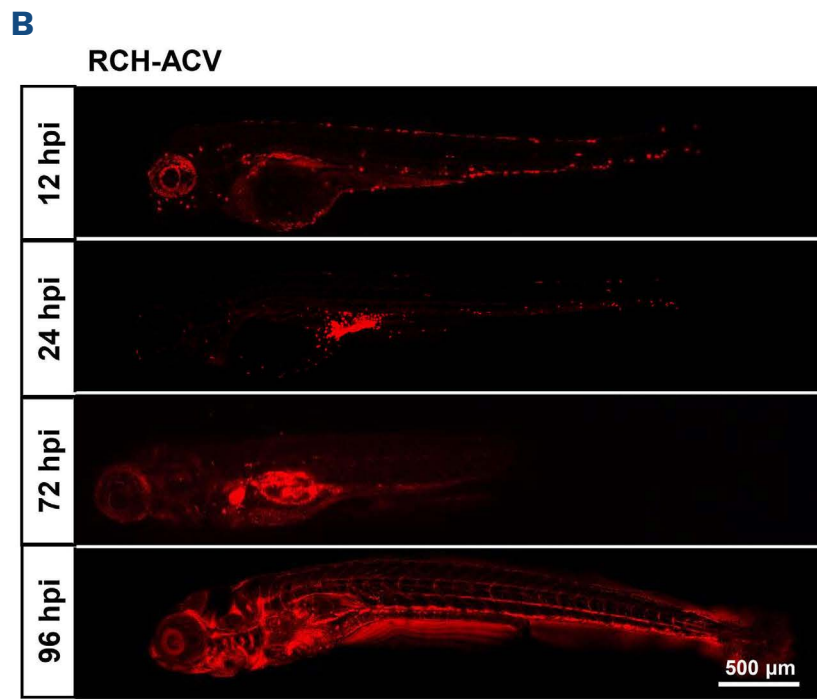
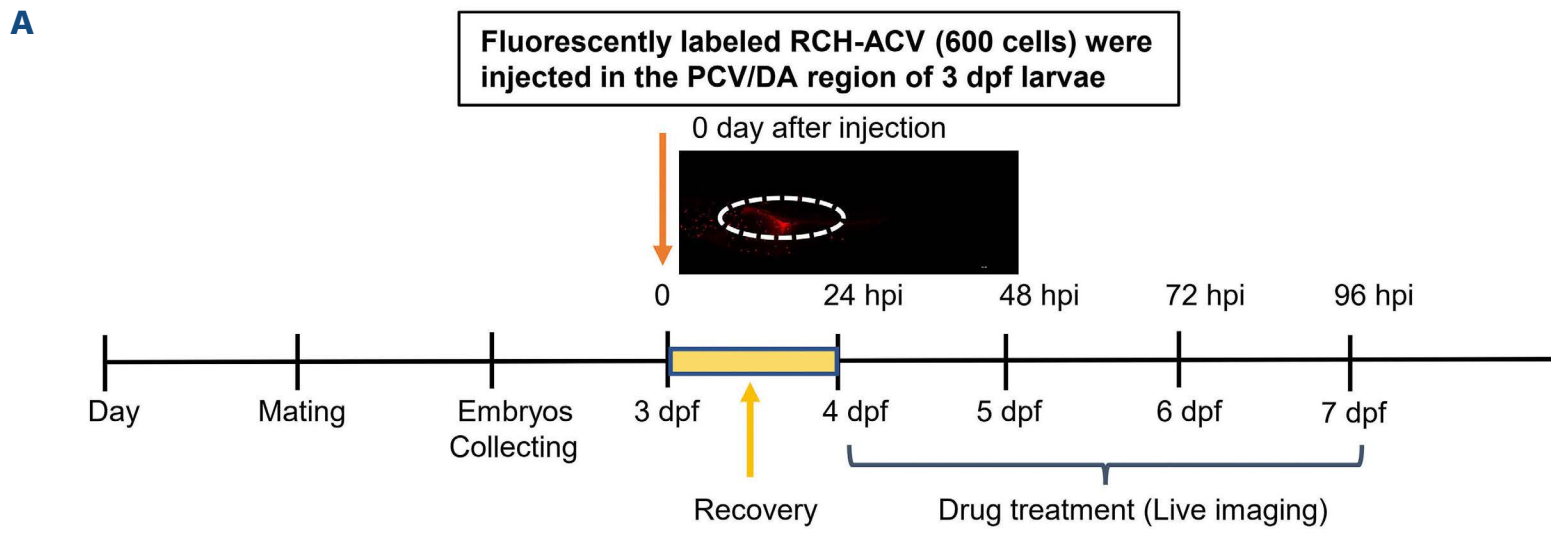


Figure 7. KJ-Pyr-9, OUL35, and CID44216842 effectively alleviate hE2A-PBX1-induced myeloid expansion in zebrafish larvae. (A) Flow-chart illustrating the high-throughput drug screening process conducted in this study. Briefly, embryos were collected and subjected to a 1-hour heat shock at 12 hours post-fertilization (hpf), followed by twice daily 2-hour heat shocks from 1 to 3 days post-fertilization (dpf). Subsequently, zebrafish larvae were soaked in a solution containing small molecule compounds (initial screening concentration was 12 μ M), the number of neutrophils was quantified using Sudan Black B (SB) staining at 6 dpf. (B) SB staining of sibling (left panel) and *Tg(hsp70:E2A-PBX1-EGFP)* (right panel) larvae after treatment with dimethyl sulfoxide (DMSO), 6.17 mM Ara-C (cytarabine), 8 μ M KJ-Pyr-9, 20 μ M CID44216842 and 24 μ M of OUL35 at 6 dpf. (B') Statistical analysis of the SB⁺ signals shown in panel (B). The black asterisks indicate statistical difference (N \geq 18, one-way ANOVA, mean \pm standard error of the mean [SEM]; * P <0.05, *** P <0.001). (C) SB staining of hE2A-PBX1 zebrafish larvae after inhibitors treatment (DMSO, 500 μ M pomalidomide, 500 μ M lenalidomide, and 0.75 μ M Y-320 inhibitor, respectively). The caudal hematopoietic tissue (CHT) is enlarged in the red box (original magnification \times 200). (C') Statistical analysis of the SB⁺ signals in panel (C). The black asterisks indicate statistical difference (N \geq 18, one-way ANOVA, mean \pm SEM; ** P <0.01, **** P <0.0001). (D) Real time quantitative polymerase chain reaction (RT-qPCR) analysis showing mRNA expression of *mmp13*, *fosab*, *hsp27*, *junb*, *mmp9*, and *fosl1* in *Tg(hsp70:E2A-PBX1-EGFP)* compared to siblings after inhibitor treatment (one-way ANOVA, mean \pm SEM; * P <0.05, *** P <0.001, **** P <0.0001). (E) Schematic representation of inhibitors targeting TNF/IL-17/MAPK signaling pathway. TNF: tumor necrosis factor; IL-17: interleukin-17; MAPK: mitogen-activated protein kinase. The AP-1 (activator protein 1) transcription factor is a dimeric complex that contains members of the JUN, FOS, ATF and MAF protein families.

The results showed that TNF and IL-17 inhibitors did not activate phosphorylation levels of Erk, Akt, p-38, and Jnk in the MAPK pathway (Online Supplementary Figure S7D, D'). However, they did decrease the expression of the target gene

mmp13, *fosab*, *mmp9* and *fosl1*, and finally alleviate myeloid cell proliferation in hE2A-PBX1 zebrafish (Figure 7C, D). These data suggest that TNF and IL-17 regulate myeloid development by upregulating the expression of target genes, not through



Continued on following page.

Figure 8. KJ-Pyr-9, OUL35 and CID44216842 effectively inhibit the oncogenicity of human E2A-PBX1-associated pre-B-lineage acute lymphoblastic leukemia. (A) Schematic representation of xenograft development using human B-lineage acute lymphoblastic leukemia (B-ALL) *E2A-PBX1(+)* RCH-ACV cells in zebrafish larvae. Briefly, embryos were injected with 600 fluorescently labeled RCH-ACV cells into the posterior cardinal vein (PCV) or dorsal aorta (DA) at 3 days post-fertilization (dpf), followed by treatment with small molecules at 24 hours post-injection (hpi). The pre-B ALL cells injected in *runx1^{w84x}* embryos were monitored by imaging at 12 hpi, 24 hpi, 72 hpi and 96 hpi. (B) RCH-ACV cells were calculated after xenografting into *runx1^{w84x}* zebrafish at 12 hpi, 24 hpi, 72 hpi and 96 hpi. (B') Statistical analysis of the RCH-ACV cell number after injecting in panel (B). The black asterisks indicate statistical difference ($N \geq 11$, one-way ANOVA, mean \pm standard error of the mean; $**P < 0.01$, $****P < 0.0001$). (C) RCH-ACV cells were calculated after xenografting into *runx1^{w84x}* zebrafish, followed by treatment with dimethyl sulfoxide (DMSO), 6.17 mM Ara-C (cytarabine), 8 μ M KJ-Pyr-9, 20 μ M CID44216842 and 24 μ M OUL35 at 96 hpi. (C') Statistical analysis of the RCH-ACV cell number with drug treatment after injecting in panel (C). The black asterisks indicate statistical difference ($N \geq 10$, one-way ANOVA, mean \pm standard error of the mean; $***P < 0.001$, $****P < 0.0001$).

the activation of the MAPK signaling pathway (Figure 7E).

KJ-Pyr-9, OUL35 and CID44216842 effectively inhibit the oncogenicity of human E2A-PBX1-associated pre-B lineage acute lymphoblastic leukemia

Considering that hE2A-PBX1 can promote pre-B ALL by upregulating *RUNX1* expression, we further verified whether KJ-Pyr-9, OUL35, and CID44216842 could also alleviate human pre-B-ALL with E2A-PBX1. We treated RCH-ACV cells with cytarabine, KJ-Pyr-9, OUL35, and CID44216842 for 60 hours, followed by assessing cell proliferation using the CCK-8 assay and apoptosis with the TUNEL assay. The results demonstrated that cytarabine, as well as these three small molecule compounds, significantly inhibited the proliferation of RCH-ACV cells and increased apoptosis in these cells (*Online Supplementary Figure S8A, B*). This suggests that the E2A-PBX1⁺ B-ALL cell line (RCH-ACV) is sensitive to these three small molecule inhibitors. We stained RCH-ACV with the lipophilic dye Dil and microinjected it at a concentration of 600 cells per embryo into posterior cardinal vein (PCV) or DA sites in immunodeficient *runx1^{w84x}* fish at 3 dpf (Figure 8A). Drug treatment was performed on the day after injection (24 hpi), and the number of leukemia cells was counted at 12–96 hpi. Our findings revealed that DMSO-treated zebrafish showed rapid expansion of RCH-ACV cells at 24–96 hpi (Figure 8B), whereas treatment with OUL35, KJ-Pyr-9, and CID44216842 inhibited the high-speed expansion of RCH-ACV cells (Figure 8C). These data suggest that KJ-Pyr-9, OUL35 and CID44216842 can effectively inhibit the oncogenicity of human E2A-PBX1-associated pre-B ALL.

Discussion

In summary, we developed a hE2A-PBX1 transgenic zebrafish line that can induce myeloid expansion and eventual progression to AML-like hemogram. We found that hE2A-PBX1 induces upregulation of the *runx1*-activated TNF/IL-17/MAPK signaling pathway. Through high-throughput drug screening and validation, we identified compounds KJ-Pyr-9, OUL35 and CID44216842 that can alleviate hE2A-PBX1-induced AML-like disease in zebrafish as well as the human pre-B ALL. Our study highlights the potential of these compounds as targeted

drugs for the future clinical treatment of E2A-PBX1 leukemia. Clinically, hE2A-PBX1 primarily induces ALL, but in our hE2A-PBX1 zebrafish model, it causes myeloid leukemia. There are two possible explanations for this: i) impaired E2A function: E2A plays a critical role in regulating early B-cell development and can enhance B-cell-specific gene transcription even in non-lymphoid cells.¹⁴⁸ The fusion gene hE2A-PBX1 disrupts the normal structure and function of WT E2A, resulting in E2A dosage and functional defects. This disruption leads to aberrant B-cell development and differentiation. Notably, in our hE2A-PBX1 transgenic fish, the endogenous *e2a* structure remains intact with normal expression levels, indicating a distinction from human cases. ii) Expression distribution of hE2A-PBX1 in different blood lineages: in patients, the expression of hE2A-PBX1 is controlled by the endogenous *E2A* promoter, implying that lymphocytes may exhibit higher expression levels of hE2A-PBX1 compared to other blood cells. The lymphoid lineage, with relatively higher expression of hE2A-PBX1, might be more prone to leukemic transformation. In our transgenic fish, hE2A-PBX1 was expressed at the initial stage of hematopoiesis (HSPC cells) through heat shock induction. This led to elevated expression of *Runx1* in HSPC, ultimately allowing HSPC to acquire a propensity for myeloid differentiation and the potential for myeloid expansion. It is important to note that the induction of both lymphoid and myeloid leukemogenesis by hE2A-PBX1 is strongly correlated with heightened *Runx1* activity, as supported by our findings and previous studies.¹⁴⁹ Inhibiting the abnormal activation of *RUNX1* and its downstream pathways shows promise as a potential shared therapeutic strategy for treating E2A-PBX1 multitype leukemia.

Based on previous structural and molecular functional studies, there are three main explanations for the potential mechanisms underlying hE2A-PBX1-induced pre-B leukemia:²¹ i) The fusion gene hE2A-PBX1 impairs the function of WT E2A; ii) hE2A-PBX1 oncoprotein may deregulate the expression of critical genes normally controlled by PBX/HOX/MEINOX complexes; and iii) hE2A-PBX1 alters the function of transcriptional co-activators, such as histone acetyltransferases p300 and CREB-binding protein (CBP). These three factors may coordinate and regulate the occurrence of hE2A-PBX1 pre-B leukemia. On the one hand,

the insufficient dose of WT E2A affects the regulation of lymphangiogenesis development.^{50,51} On the other hand, hE2A-PBX1 induces oncogenic properties, such as cell proliferation, by altering the expression of downstream genes or transcriptional co-activators of PBX1.⁵² In our study, the induction of hE2A-PBX1 expression, along with the regular expression of the endogenous *E2A* gene, leads to the development of myeloid leukemia. This suggests that the acquired function of hE2A-PBX1, rather than a deficiency of WT E2A, is the primary cause of its carcinogenic potential. However, disruption of the *E2A* gene may contribute to alterations in lymphoid development. Consistent with this, an unbiased analysis of E2A-PBX1 cistrome in pre-B ALL cells reveals that E2A-PBX1 can interact with RUNX1, resulting in transcriptome alterations, including activation of RUNX1 itself.¹ Moreover, our study revealed aberrant activation of Runx1 in hE2A-PBX1 transgenic fish. Notably, inhibiting Runx1 and its downstream pathway demonstrated significant alleviation in the expansion of leukemic cells in both zebrafish and human cell lines. These findings emphasize that hE2A-PBX1 exerts a significant impact on tumorigenesis by regulating the genome through direct binding with RUNX1. Whether this effect is synergistically facilitated by the inappropriate activation of target genes through the fusion of PBX1 DNA binding motifs remains to be further investigated.

Currently, there are no clinically targeted drugs for the treatment of E2A-PBX1 leukemia, and there are relatively few studies on the treatment of E2A-PBX1-associated AML-like disease and MPAL. In this study, we show that the small molecule compounds KJ-Pyr-9, OUL35 and CID44216842 obtained by hE2A-PBX1 zebrafish leukemia model have great potential. OUL35, recognized as a selective PARP inhibitor that targets PKC δ , a PARP substrate that activates MAPK,^{53,54} has demonstrated the ability to protect HeLa cells from ARTD10-induced cell death.⁵⁵ KJ-Pyr-9 is an inhibitor of MYC,⁵⁶ a transcriptional regulatory factor encoded by the common proto-oncogene MYC, which mainly exerts its regulatory effects through binding with MAX protein.⁵⁷ Notably, the expression of *max* was significantly increased in hE2A-PBX1 zebrafish (*data not shown*). Literature reports indicate that KJ-Pyr-9 can target MYC to inhibit pleomorphic glioblastoma multiforme (GBM) and significantly reduce the viability of squamous cell carcinoma (SCC) and adenocarcinoma (AC)-derived cells.⁵⁸ CID44216842 acts as an inhibitor of RAS, a key regulator of signaling pathways controlling normal cell growth and malignant transformation. Additionally, CID44216842 has been demonstrated to inhibit stimulus-induced Cdc42 activation

in Swiss 3T3 fibroblasts.⁵⁹ While *in vitro* cellular experiments confirm their efficacy in tumor cell therapy, it is essential to conduct experiments using animal tumor models before progressing to clinical trials. In our study, these three small molecule compounds exhibit the ability to alleviate hE2A-PBX1-induced AML-like disease in zebrafish as well as pre-B ALL associated with hE2A-PBX1, by targeting the TNF/IL-17/MAPK pathway downstream of Runx1. However, it is not clear whether these small molecule compounds are applicable to other blood diseases with abnormal RUNX1 activity, and more preclinical animal studies are needed to confirm this. Overall, our findings shed new light on the treatment of E2A-PBX1 and other Runx1-related disorders. Although there is much work to be done, we anticipate that our research will contribute to the development of innovative therapeutic strategies for these diseases.

Disclosures

No conflicts of interest to disclose.

Contributions

WL and WZ conceived and supervised the study and edited the article. HL and QL performed experiments and wrote, reviewed, and edited the article. JH, WD, KW, SL, and HW performed the experiments. ZH reviewed and edited the article.

Acknowledgments

The authors would like to thank Dr. Huafeng Xie for providing RCH-ACV cells. The authors would like to thank Dr. Kailun Li, Dr. Xiao Fang, Dr. Panpan Zhu, Dr. Shuang Zhao and Dr. Zhibin Huang for their helpful suggestions.

Funding

This work was supported by the National Natural Science Foundation of China (82070163), Guangdong Basic and Applied Basic Research Foundation (2020A1515011218) and Special Fund of Science and Technology Innovation Cultivation for College Students in Guangdong Province (pd-jh2020b0048).

Data-sharing statement

The data supporting the findings of this study are available within the article and its Online Supplementary Appendix. Data produced in this manuscript are available on Gene Expression Omnibus (GEO) with accession number GSE234222 (Go to <https://www.ncbi.nlm.nih.gov/geo/query/acc.cgi?acc=GSE234222>, enter the token qjebmoqwprsjtkn into the box).

References

1. Pi W-C, Wang J, Shimada M, et al. E2A-PBX1 functions as a coactivator for RUNX1 in acute lymphoblastic leukemia. *Blood*. 2020;136(1):11-23.
2. Duque-Afonso J, Lin CH, Han K, et al. E2A-PBX1 remodels oncogenic signaling networks in B-cell precursor acute lymphoid leukemia. *Cancer Res*. 2016;76(23):6937-6949.

3. Amor Vigil AM, Fernández Martínez L, Díaz Alonso CA, et al. Transcripto E2A-PBX1 en paciente pediátrico con leucemia aguda híbrida linfoide b/mieloide. *Rev Cubana Hematol Inmunol Hemoter.* 2017;33(3):95-101.
4. Troussard X, Rimokh R, Valensi F, et al. Heterogeneity of t(1;19) (q23;p13) acute leukaemias. French Haematological Cytology Group. *Br J Haematol.* 1995;89(3):516-526.
5. Hong Y, Zhao X, Qin Y, et al. The prognostic role of E2A-PBX1 expression detected by real-time quantitative reverse transcriptase polymerase chain reaction (RQ-PCR) in B cell acute lymphoblastic leukemia after allogeneic hematopoietic stem cell transplantation. *Ann Hematol.* 2018;97(9):1547-1554.
6. Irving JAE, Enshaei A, Parker CA, et al. Integration of genetic and clinical risk factors improves prognostication in relapsed childhood B-cell precursor acute lymphoblastic leukemia. *Blood.* 2016;128(7):911-922.
7. Hunger SP. Chromosomal translocations involving the E2A gene in acute lymphoblastic leukemia: clinical features and molecular pathogenesis. *Blood.* 1996;87(4):1211-1224.
8. Zhao W, Li Z-g, Gao C. Detection of E2A/PBX1 fusion gene and its clinical significance in childhood acute lymphoblastic leukemia. *Zhonghua Er Ke Za Zhi.* 2008;46(7):550-551.
9. Jia M, Hu B-F, Xu X-J, Zhang J-Y, Li S-S, Tang Y-M. Clinical features and prognostic impact of TCF3-PBX1 in childhood acute lymphoblastic leukemia: a single-center retrospective study of 837 patients from China. *Curr Probl Cancer.* 2021;45(6):100758.
10. Diakos C, Xiao Y, Zheng S, Kager L, Dworzak M, Wiemels JL. Direct and indirect targets of the E2A-PBX1 leukemia-specific fusion protein. *PLoS One.* 2014;9(2):e87602.
11. Murre C. Regulation and function of the E2A proteins in B cell development. In: Gupta S, Alt F, Cooper M, Melchers F, Rajewsky K, eds. *Mechanisms of lymphocyte activation and immune regulation XI.* B Cell Biology. Boston, MA: Springer; 2007. p. 1-7.
12. Semerad CL, Mercer EM, Inlay MA, Weissman IL, Murre C. E2A proteins maintain the hematopoietic stem cell pool and promote the maturation of myelolymphoid and myeloerythroid progenitors. *Proc Natl Acad Sci U S A.* 2009;106(6):1930-1935.
13. Malouf C, Ottersbach K. Molecular processes involved in B cell acute lymphoblastic leukaemia. *Cell Mol Life Sci.* 2018;75(3):417-446.
14. Aspland SE, Bendall HH, Murre C. The role of E2A-PBX1 in leukemogenesis. *Oncogene.* 2001;20(40):5708-5717.
15. Kamps MP, Baltimore D. E2A-Pbx1, the t(1;19) translocation protein of human pre-B-cell acute lymphocytic leukemia, causes acute myeloid leukemia in mice. *Mol Cell Biol.* 1993;13(1):351-357.
16. Kamps MP, Wright DD. Oncoprotein E2A-Pbx1 immortalizes a myeloid progenitor in primary marrow cultures without abrogating its factor-dependence. *Oncogene.* 1994;9(11):3159-3166.
17. Dederda DA, Waller EK, LeBrun DP, et al. Chimeric homeobox gene E2A-PBX1 induces proliferation, apoptosis, and malignant lymphomas in transgenic mice. *Cell.* 1993;74(5):833-843.
18. Bijl J, Sauvageau M, Thompson A, Sauvageau G. High incidence of proviral integrations in the Hoxa locus in a new model of E2a-PBX1-induced B-cell leukemia. *Genes Dev.* 2005;19(2):224-233.
19. Sera Y, Yamasaki N, Oda H, et al. Identification of cooperative genes for E2A-PBX1 to develop acute lymphoblastic leukemia. *Cancer Sci.* 2016;107(7):890-898.
20. Sykes DB, Kamps MP. E2a/Pbx1 induces the rapid proliferation of stem cell factor-dependent murine pro-t cells that cause acute T-lymphoid or myeloid leukemias in mice. *Mol Cell Biol.* 2004;24(3):1256-1269.
21. Hyndman BD, LeBrun DP. E2A-PBX1. In: Schwab, M. (eds) *Encyclopedia of cancer.* Springer, Berlin, Heidelberg; 2009. p. 935-936.
22. van de Ven C, Boeree A, Stalpers F, Zwaan CM, Den Boer ML. Ibrutinib is not an effective drug in primografts of TCF3-PBX1. *Transl Oncol.* 2020;13(10):100817.
23. Eldfors S, Kuusanmaki H, Kontro M, et al. Idelalisib sensitivity and mechanisms of disease progression in relapsed TCF3-PBX1 acute lymphoblastic leukemia. *Leukemia.* 2017;31(1):51-57.
24. Rasighaemi P, Basheer F, Liongue C, Ward AC. Zebrafish as a model for leukemia and other hematopoietic disorders. *J Hematol Oncol.* 2015;8(1):1-10.
25. Ali S, Champagne DL, Spaink HP, Richardson MK. Zebrafish embryos and larvae: a new generation of disease models and drug screens. *Birth Defects Res C Embryo Today.* 2011;93(2):115-133.
26. Bentley VL, Veinotte CJ, Corkery DP, et al. Focused chemical genomics using zebrafish xenotransplantation as a pre-clinical therapeutic platform for T-cell acute lymphoblastic leukemia. *Haematologica.* 2015;100(1):70-76.
27. Haney MG, Moore LH, Blackburn JS. Drug screening of primary patient derived tumor xenografts in zebrafish. *J Vis Exp.* 2020(158):10.
28. Chauvigné F, Yilmaz O, Ferré A, et al. The vertebrate Aqp14 water channel is a neuropeptide-regulated polytransporter. *Commun Biol.* 2019;2(1):462.
29. Jin H, Sood R, Xu J, et al. Definitive hematopoietic stem/progenitor cells manifest distinct differentiation output in the zebrafish VDA and PBI. *Development.* 2009;136(4):647-654.
30. Jin H, Li L, Xu J, et al. Runx1 regulates embryonic myeloid fate choice in zebrafish through a negative feedback loop inhibiting Pu.1 expression. *Blood.* 2012;119(22):5239-5249.
31. Pruvot B, Jacquelin A, Droin N, et al. Leukemic cell xenograft in zebrafish embryo for investigating drug efficacy. *Haematologica.* 2011;96(4):612-616.
32. Zeng Y, Zhang X, Lin D, et al. A lysosome-targeted dextran-doxorubicin nanodrug overcomes doxorubicin-induced chemoresistance of myeloid leukemia. *J Hematol Oncol.* 2021;14(1):1-6.
33. Khan N, Mahajan NK, Sinha P, Jayandharan GR. An efficient method to generate xenograft tumor models of acute myeloid leukemia and hepatocellular carcinoma in adult zebrafish. *Blood Cells Mol Dis.* 2019;75:48-55.
34. Xu J, Du L, Wen Z. Myelopoiesis during zebrafish early development. *J Genet Genomics.* 2012;39(9):435-442.
35. LeBrun DP. E2A basic helix-loop-helix transcription factors in human leukemia. *Front Biosci.* 2003;8:s206-s222.
36. Baker WJ, Royer GL, Jr., Weiss RB. Cytarabine and neurologic toxicity. *J Clin Oncol.* 1991;9(4):679-693.
37. Ota K. [Cytarabine]. *Gan To Kagaku Ryoho.* 1987;14(10):2983-2987. Japanese.
38. Magina KN, Pregartner G, Zebisch A, et al. Cytarabine dose in the consolidation treatment of AML: a systematic review and meta-analysis. *Blood.* 2017;130(7):946-948.
39. Zeidner JF, Karp JE. Clinical activity of alvocidib (flavopiridol) in acute myeloid leukemia. *Leuk Res.* 2015;39(12):1312-1318.
40. Chen KTJ, Militao GGC, Anantha M, Witzigmann D, Leung AWY, Bally MB. Development and characterization of a novel flavopiridol formulation for treatment of acute myeloid leukemia. *J Control Release.* 2021;333:246-257.
41. Sood R, Kamikubo Y, Liu P. Role of RUNX1 in hematological malignancies. *Blood.* 2017;129(15):2070-2082.

42. Yan Z, Dai J, Wang J, et al. RNF167-mediated ubiquitination of Tollip inhibits TNF- α -triggered NF- κ B and MAPK activation. *FASEB J*. 2023;37(8):e23089.
43. Niu L, Fang Y, Yao X, et al. TNF α activates MAPK and Jak-Stat pathways to promote mouse Muller cell proliferation. *Exp Eye Res*. 2021;202:108353.
44. Sabio G, Davis RJ. TNF and MAP kinase signalling pathways. *Semin Immunol*. 2014;26(3):237-245.
45. Aslani MR, Sharghi A, Boskabady MH, et al. Altered gene expression levels of IL-17/TRAF6/MAPK/USP25 axis and pro-inflammatory cytokine levels in lung tissue of obese ovalbumin-sensitized rats. *Life Sci*. 2022;296:120425.
46. Roussel L, Houle F, Chan C, et al. IL-17 Promotes p38 MAPK-dependent endothelial activation enhancing neutrophil recruitment to sites of inflammation. *J Immunol*. 2010;184(8):4531-4537.
47. Hata K, Andoh A, Shimada M, et al. IL-17 stimulates inflammatory responses via NF- κ B and MAP kinase pathways in human colonic myofibroblasts. *Am J Physiol Gastrointest Liver Physiol*. 2002;282(6):G1035-G1044.
48. Sloan SR, Shen CP, McCarrick-Walmsley R, Kadesch T. Phosphorylation of E47 as a potential determinant of B-cell-specific activity. *Mol Cell Biol*. 1996;16(12):6900-6908.
49. Licht JD. Oncogenesis by E2A-PBX1 in ALL: RUNX and more. *Blood*. 2020;136(1):3-4.
50. Huang A, Zhao H, Quan Y, Jin R, Feng B, Zheng M. E2A Predicts prognosis of colorectal cancer patients and regulates cancer cell growth by targeting miR-320a. *Plos One*. 2014;9(1):e85201.
51. Xu W, Carr T, Ramirez K, McGregor S, Sigvardsson M, Kee BL. E2A transcription factors limit expression of Gata3 to facilitate T lymphocyte lineage commitment. *Blood*. 2013;121(9):1534-1542.
52. Lu Q, Kamps MP. Selective repression of transcriptional activators by Pbx1 does not require the homeodomain. *Proc Natl Acad Sci U S A*. 1996;93(1):470-474.
53. Mandal JP, Shiue C-N, Chen Y-C, et al. PKC δ mediates mitochondrial ROS generation and oxidation of HSP60 to relieve RKIP inhibition on MAPK pathway for HCC progression. *Free Radic Biol Med*. 2021;163:69-87.
54. Tian Y, Korn P, Tripathi P, et al. The mono-ADP-ribosyltransferase ARTD10 regulates the voltage-gated ion channel Kv1.1 through protein kinase C delta. *BMC Biol*. 2020;18(1):143.
55. Murthy S, Desantis J, Verheugd P, et al. 4-(Phenoxy) and 4-(benzyloxy)benzamides as potent and selective inhibitors of mono-ADP-ribosyltransferase PARP10/ARTD10. *Eur J Med Chem*. 2018;156:93-102.
56. Hart JR, Garner AL, Yu J, et al. Inhibitor of MYC identified in a Krohnke pyridine library. *Proc Natl Acad Sci U S A*. 2014;111(34):12556-12561.
57. Lourenco C, Resetca D, Redel C, et al. MYC protein interactors in gene transcription and cancer. *Nat Rev Cancer*. 2021;21(9):579-591.
58. Windmoeller BA, Beshay M, Helweg LP, et al. Novel primary human cancer stem-like cell populations from non-small cell lung cancer: inhibition of cell survival by targeting NF- κ B and MYC signaling. *Cells*. 2021;10(5):1024.
59. Hong L, Kenney SR, Phillips GK, et al. Characterization of a Cdc42 protein inhibitor and its use as a molecular probe. *J Biol Chem*. 2013;288(12):8531-8543.